INFORMATION TO USERS

This manuscript has been reproduced from the microfilm master. UMI films the text directly from the original or copy submitted. Thus, some thesis and dissertation copies are in typewriter face, while others may be from any type of computer printer.

The quality of this reproduction is dependent upon the quality of the copy submitted. Broken or indistinct print, colored or poor quality illustrations and photographs, print bleedthrough, substandard margins, and improper alignment can adversely affect reproduction.

In the unlikely event that the author did not send UMI a complete manuscript and there are missing pages, these will be noted. Also, if unauthorized copyright material had to be removed, a note will indicate the deletion.

Oversize materials (e.g., maps, drawings, charts) are reproduced by sectioning the original, beginning at the upper left-hand corner and continuing from left to right in equal sections with small overlaps.

Photographs included in the original manuscript have been reproduced xerographically in this copy. Higher quality 6" x 9" black and white photographic prints are available for any photographs or illustrations appearing in this copy for an additional charge. Contact UMI directly to order.

Bell & Howell Information and Learning
300 North Zeeb Road, Ann Arbor, MI 48106-1346 USA

UMI®
800-521-0600

Single Label Fluorescent Derivatization of Peptides

Michael J. Little

A Thesis

In

The Department

of

Chemistry and Biochemistry

Presented In Partial Fulfillment of the Requirements
for the Degree of Master of Science
Concordia University
Montreal, Quebec

April, 1997

ABSTRACT

Single Label Fluorescent Derivatization of Peptides

Michael J. Little

A one step method for the attachment of a single fluorescent label to peptides through their N-terminus is described. The method employs fluorescein-5-isothiocyanate as the label of choice and a lower than normal derivatization buffer pH that discriminates against ε-amino derivatization in favor of α-amino derivatization provided that this group may act as an efficient nucleophile. A kinetic study was performed in order to identify the optimal derivatization buffer pH for α-amino group selectivity, using Nα-t-BOC-L-lysine and Nε-t-BOC-L-lysine as model compounds for derivatization through ε-amino and α-amino groups, respectively. The optimal pH was found to be 8.5. Six small peptides, Arg-Lys, Lys-Trp-Lys, Lys-Lys, Lys-Lys-Lys, Lys-Lys-Lys-Lys and Arg-Pro-Lys-Pro, were derivatized at pH 8.5 in an effort to corroborate the results of the kinetic study. It was found that this method of single label derivatization via buffer pH control was successful for peptides with fewer than four lysines residues.

ACKNOWLEDGMENTS

I would like to thank my supervisor, Dr. Peter Banks, for allowing me the opportunity to work in his laboratory and become a part of his research environment. It has truly been a joy to work for Peter and I am ever grateful for his invaluable encouragement, thoughtfulness, assistance and advice throughout this work and the writing of this thesis. Without Peter I would not have come as far as I have.

I would also like to thank Donald Paquette and Michael Harvey for providing a wonderful working atmosphere, countless inspirations and helpful advice. The "Group Meetings" at Hurley's will always live with me. I would also like to thank Michael for assisting in the collection of some of the data for this project (it was a nice vacation) and Donald for setting up and teaching me how to use our CE-LIF system.

Special thanks to:

- Dr. English and her lab group for their assistance and use of equipment from time to time. In addition, I would like to thank Dr. English for her occasional assistance and for her presence on my committee.
- Dr. Joanne Turnbull for her presence on my committee and also for teaching me that enzymes are not just "E", substrates are not just "S" and products are not just "P". They can be other letters too. (Just kidding)
- "The girls next door", Kelly and Suzanne, for coffee breaks, lunch, and helping Donald and Michael keep me sane.
- Fabian Zaccardo, Honghao Zhang and Wenbin Zhang for technical assistance.
- My parents, Dolores and Bernie, and my sister and bother-in-law, Susan and Ed, for providing me with financial aid and moral support whenever it was necessary.

and finally I would like to thank Gia Klironomos for her support, encouragement, patience and presence during this last year of my degree and also her family for their kindness, many meals and lunches, and for being my family away from home.

TABLE OF CONTENTS

List of Figures

List of Tables

Abbreviations

CEC	Capillary Electrokinetic Chromatography
CE	Capillary Electrophoresis
CGE	Capillary Gel Electrophoresis
CIEF	Capillary Isoelectric Focusing
CZE	Capillary Zone Electrophoresis
CFSE	Carboxyfluorescein Succinimidyl Ester
DMF	N,N-Dimethylformamide
EOF	Electroosmotic Flow
ESI-MS	Electrospray-Ionization Mass Spectrometry
DTAF	Fluorescein Dichlorotriazine
FITC	Fluorescein Isothiocyanate
FL	Focal Length
GC	Gas Chromatography
HPLC	High Performance Liquid Chromatography

IHP	Inner Helmholtz Plane
i.d.	Internal Diameter
LIF	Laser-Induced Fluorescence
LOD	Limit of Detection
MECC	Micellar Electrokinetic Capillary Chromatography
NA	Numerical Aperture
o.d.	Outer Diameter
OHP	Outer Helmholtz Plane
PITC	Phenyl Isothiocyanate
PMT	Photomultiplier Tube
t-BOC	*tert*-Butoxycarbonyl
WD	Working Distance

CHAPTER 1

INTRODUCTION TO CAPILLARY ELECTROPHORESIS WITH LASER INDUCED FLUORESCENCE DETECTION

1.1 Open Tubular Electrophoresis

The goal of many analytical chemists is to determine various qualitative and quantitative aspects of a sample. Usually there are numerous analysis techniques available depending on the nature of the sample and what is to be quantified. A quick review of virtually any analytical chemistry journal reveals that analytical chemists are interested in a very diverse range of analyses, such as that of raindrops [1], foods [2], and drug-protein interactions [3], to name a few. Given that most real samples contain many different compounds, it is not surprising that some of the premier analysis methods involve separations. There are a number of available separation methodologies, including: high performance liquid chromatography (HPLC), gas chromatography (GC), and gel electrophoresis. Each of these techniques have been well researched and are standard in many laboratories. Recently, however, capillary electrophoresis (CE) has become a widely accepted separation technique that may be used in the analytical laboratory. Its growing popularity stems from its ability to separate complex mixtures [4] with short analysis times [5] and high efficiencies [6], while requiring only minute amounts of sample [7].

The first column electrophoresis instrument was assembled by Hjertén in 1967 [8]. Hjertén employed a 1-3mm internal diameter (i.d.) quartz tube immersed in a cooling bath and continually rotated about its axis in order to reduce convective mixing due to the

electrically generated heat, termed Joule heating, within the tube. Joule heating occurs whenever an electric current is passed through a solution. The amount of heat generated is proportional to the applied electric field and the conductivity of the buffer while the ability of the heat to be dissipated is a function of the internal radius of the capillary and its thermal conductivity. Separations of inorganic ions and proteins demonstrated the usefulness of the technique.

For the next 12 years, column electrophoresis remained relatively unexploited, until 1979 when Mikkers *et al.* [9] revived the technique. They employed a 0.2mm i.d. polytetrafluoroethylene (teflon) capillary and performed separations of various inorganic and organic analytes. Rotation of the separation capillary was unnecessary as the small dimensions of the capillary permitted effective dissipation of the generated Joule heat. UV and conductivity detection were employed and electrodispersion was found to be the major cause of dispersion of the analytes. The separated analytes possessed efficiencies of *ca.* 10^3 theoretical plates. This work may be considered the origin of open tubular electrophoresis in a capillary format, termed capillary zone electrophoresis (CZE).

In 1981, Jorgenson and Lukacs [10,11] extrapolated the work of Mikkers to 75μm i.d. borosilicate capillaries for the separation of selected fluorescamine derivatized n-alkylamines. Each alkylamine of the six separated alkylamines differed from the other by only one methylene group, thus demonstrating the power of CZE for separating solutes with small differences in structure. The possibility for an electrically driven HPLC system was also recognized and a separation of methylanthracene and perylene in a capillary filled with a reversed phase packing was carried out with acetonitrile as the separation electrolyte (mobile phase). Efficiencies of 10^4 theoretical plates were achieved. Also separated were selected dansyl amino acids, fluorescamine derivatized

amino acids and human urine [11]. Detection was carried out on-column using a home-made fluorescence detector.

These efforts began what some have termed, "The modern era of capillary electrophoresis..." [12]. CE had been demonstrated to be a highly efficient separation technique for inorganic, organic and biological ions. However, two major problem areas existed: (1) protein samples exhibited adsorption onto the inner surface of the capillary, and (2) the detection schemes employed were not sensitive enough for the analysis of a wide range of solutes [13]. Some internal capillary coatings were investigated at that time [13] and since then protein adsorption and methods to eliminate it have received much attention [14,15]. Efforts to improve detection schemes for CE have also received considerable attention in the literature [16-19]. The small i.d. capillaries currently employed for CE analysis have 20-75μm i.d.'s, which provide small optical path lengths for on-column detection schemes, ultimately limiting the detection limits. While end-column detection methods do not suffer from this limitation, their application is also non-trivial as specialized connections and/or capillaries are required for their use.

1.1.1 Capillary Zone Electrophoresis (CZE)

Although there are many forms of CE available such as micellar electrokinetic capillary chromatography (MECC), capillary gel electrophoresis (CGE), capillary isoelectric focusing (CIEF), capillary isotachophoresis (CITP) and capillary electrokinetic chromatography (CEC), CZE is probably the most common form in use. Figure 1.1 illustrates a generic CE instrument which contains all of the basic equipment required for each of the above techniques. The instrument consists of a buffer filled capillary with each end immersed in a buffer reservoir. One reservoir is contained within an electrically

isolated box with the high voltage electrode immersed in the solution while the other reservoir contains an electrode which is held at ground. When a potential is applied via the high voltage electrode, a potential difference exists across the capillary. Under an applied electric field, the anodic end of the capillary is termed the inlet end of the capillary and the cathodic end is termed the outlet end. Sample introduction may occur at the inlet end of the capillary by either electromigration or hydrodynamic injection. Detection of the separated analytes may occur at (end-column) or near (on-column) the outlet end of the capillary.

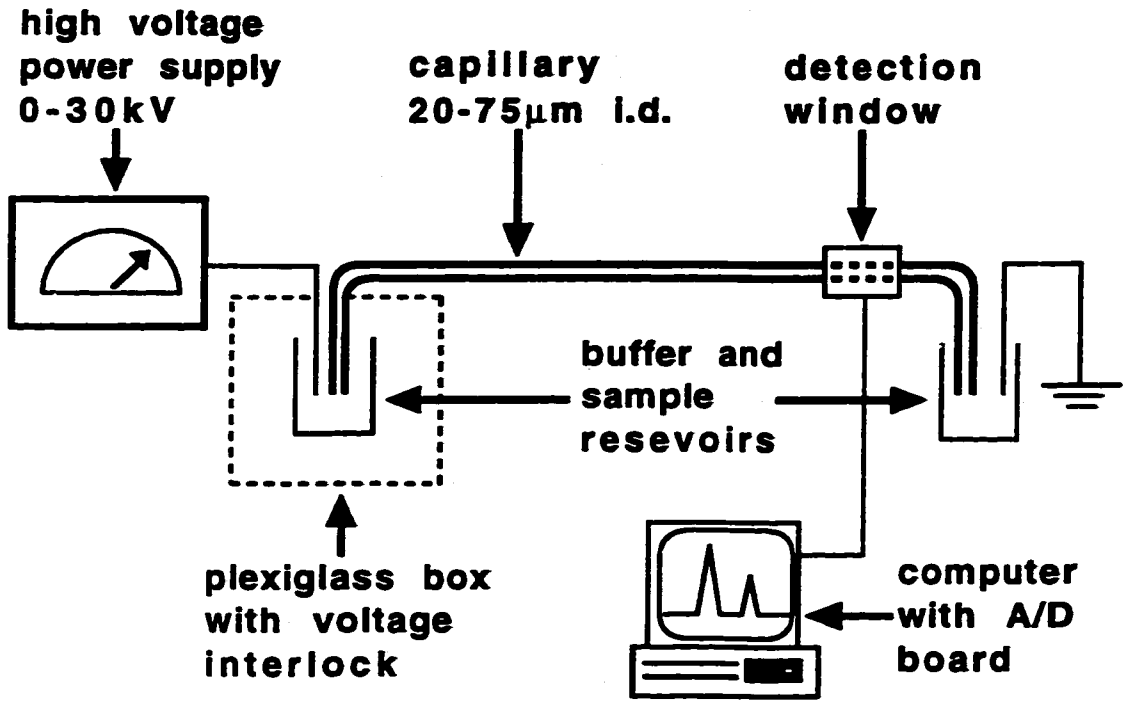

Figure 1.1: A generic capillary electrophoresis system.

1.1.2 Electroosmosis and Electroosmotic Flow (EOF)

Silica capillaries are the most commonly used capillaries for CE separations due to their heat dissipation qualities and low cost. Silicate glasses have the general structure of $(Si\text{-}O_2)_x$ and contain exposed silanol groups (Si-OH) on their surfaces. When one of these surfaces, such as the inner surface of a fused silica capillary, becomes exposed to a solution with a pH greater than *ca.* 1-1.5, some of these silanol groups become deprotonated resulting in a negative charge on the inner surface of the capillary wall [20,21]. As a result, a compact region of adsorbed ions and water molecules is formed which consists of two distinct areas, the inner Helmholtz plane (IHP) and the outer Helmholtz plane (OHP). Figure 1.2 is a representation of the electric double layer present on the inner surface of a capillary as described by Tavares and McGuffin [22]: They propose that the IHP is made up of specifically adsorbed water molecules and some electrolyte anions. The OHP consists of nonspecifically adsorbed, electrolyte cations. Random thermal motion allows these ions to diffuse a short distance into the solution, forming a diffuse layer. The point at which the charge density equals that of the bulk electrolyte, marks the edge of the bulk solution. The diffuse layer is divided into two sections by the plane of the shear. This plane separates the region of the diffuse layer which is capable of sliding past the charged capillary surface, the outer region, from that which is incapable of tangential movement, the inner region.

Under a tangential electric field the cations located outside the plane of shear are able to migrate toward the cathodic end of the capillary. The potential present at the plane of shear is termed the zeta potential, ζ.

As the bulk electrolyte is effectively in a state of electroneutrality, there is no net pull in this zone under an applied electric field. However, due to the increase in charge

density near the capillary wall, caused by the increased presence of cations, migration of this region toward the cathodic end of the capillary under an applied electric field does occur (Figure 1.3a).

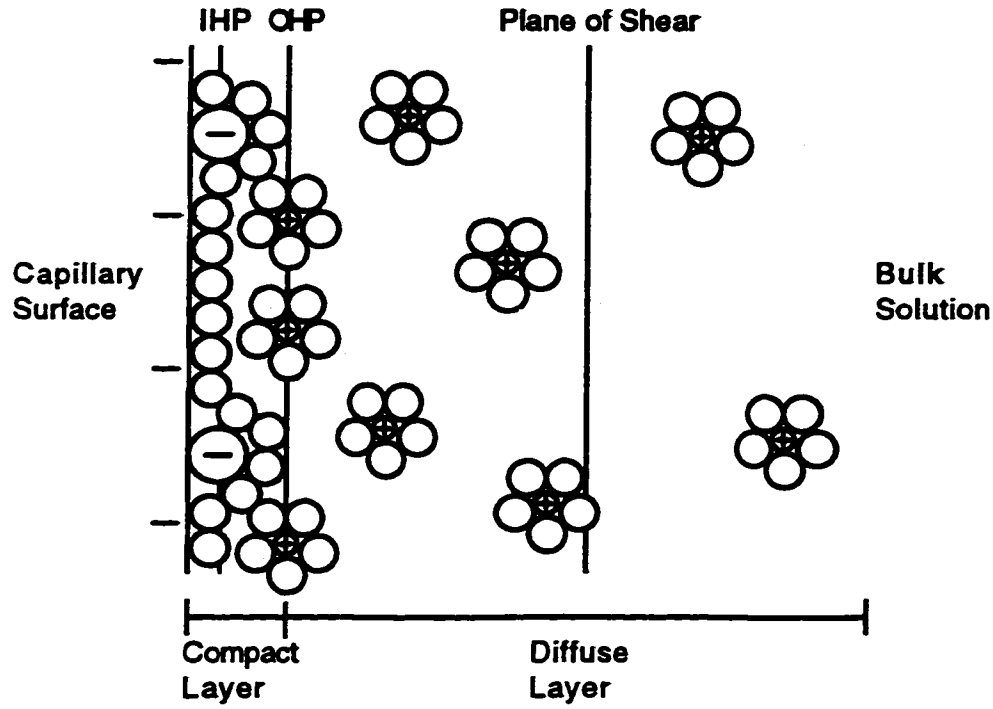

Figure 1.2: Schematic of the electric double layer present at the capillary surface. Adapted from [22].

Given that each migrating cation is solvated and an extensive hydrogen bonding network is present within the aqueous electrolyte, a net movement of the entire solution occurs toward the cathodic end of the capillary. In addition, the flow profile has a plug like shape as the pulling force is exerted at all points along the capillary wall (Figure 1.3b). This is the basis for EOF.

The velocity of the EOF is affected by the magnitude of the applied electric field, E, and the electroosmotic mobility, μ_{eo}, of the electrolyte:

$$v_{eo} = \mu_{eo} E \qquad (1.1)$$

where $E = \frac{V}{L}$, V = applied voltage, L = capillary length.

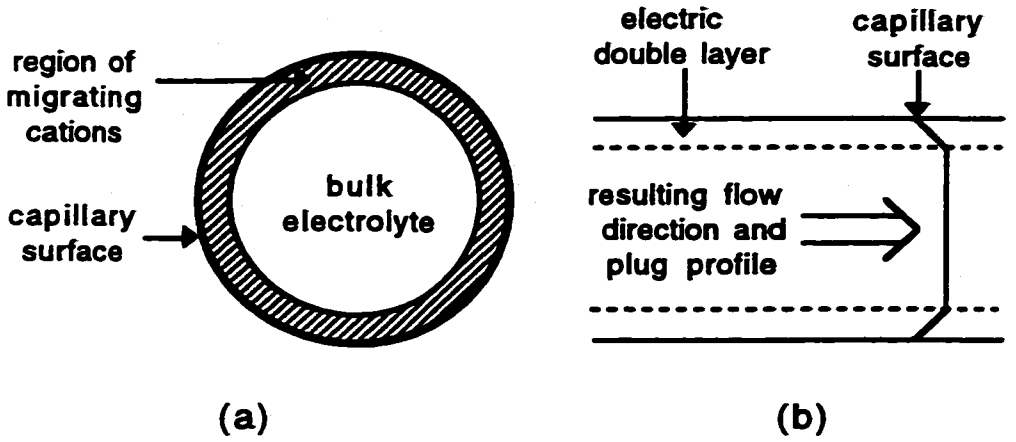

Figure 1.3: (a) Cross-section of capillary showing distribution of diffuse layer of cations.
(b) Schematic of flow direction and profile shape.

The electroosmotic mobility is specific for a given capillary type and electrolyte. It is a function of the dielectric constant, ε, and the viscosity, η, of the electrolyte, and the zeta potential, ζ.

$$\mu_{eo} = \frac{\varepsilon \zeta}{\eta} \qquad (1.2)$$

1.1.3 Electrophoretic Migration

Electrophoretic migration is the migration of a charged analyte under an applied electric field. It is dependent on the magnitude of the applied electric field and a constant, termed the electrophoretic mobility, μ_{ep}.

$$v_{ep} = \mu_{ep} E \tag{1.3}$$

The electrophoretic mobility of an ion is specific for a given analyte/electrolyte system and is directly proportional to the charge on the ion, q, and indirectly proportional to both the radius of the ion, r, and the viscosity of the solution.

$$\mu_{ep} = \frac{q}{6 \pi \eta r} \tag{1.4}$$

However, the resultant ion migration is a function of both the electrophoretic migration of the ion and that of the EOF:

$$v_{CZE} = (\mu_{eo} + \mu_{ep}) E = \mu_T E \tag{1.5}$$

where $\mu_T = \mu_{eo} + \mu_{ep}$.

Thus, provided that all anions present in a sample do not have electrophoretic mobilities greater than that of the electroosmotic mobility, all sample components will elute at the same end of the capillary (Figure 1.4).

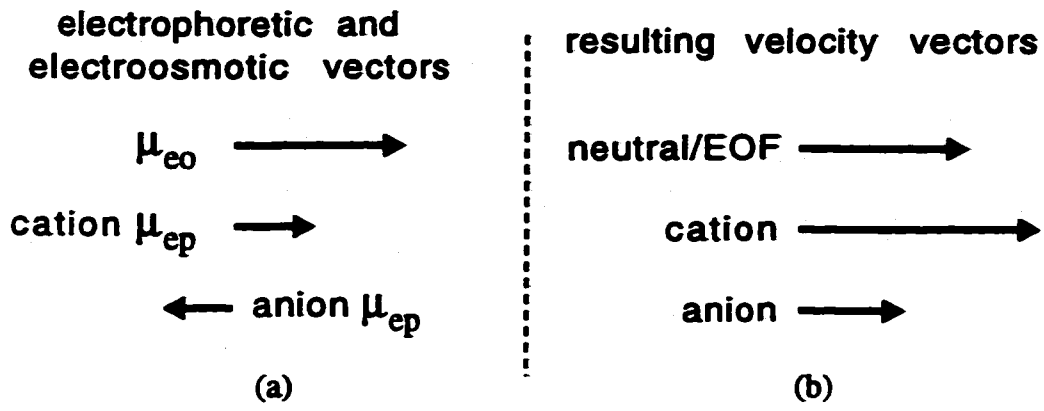

Figure 1.4: (a) Relative electrophoretic and electroosmotic vectors.
(b) Resulting velocity vectors.

1.1.4 Sources of Dispersion and Efficiency

An example of the ability of CE to separate complex samples is illustrated in Figure 1.5, where an electropherogram of a DNA sequence has been determined using CGE as the separation technique. In contrast to CGE, during a CZE analysis there no packing present within the capillary. Under ideal conditions longitudinal diffusion is the sole contributor to zone broadening. The variance introduced by longitudinal diffusion is a function of the diffusion coefficient, D, of the analyte and the time, t, spent in the capillary. With on-column detection and assuming a Gaussian peak, this is represented by:

$$\sigma^2 = 2\,D\,t = \frac{2\,D\,L_D\,L_T}{\mu_T\,V} \qquad (1.6)$$

since $v = \mu_T E = \frac{L_D}{t}$ and $E = \frac{V}{L_T}$ then $t = \frac{L_D L_T}{\mu_T V}$, where L_D = length of capillary to the detector, L_T = total length of capillary.

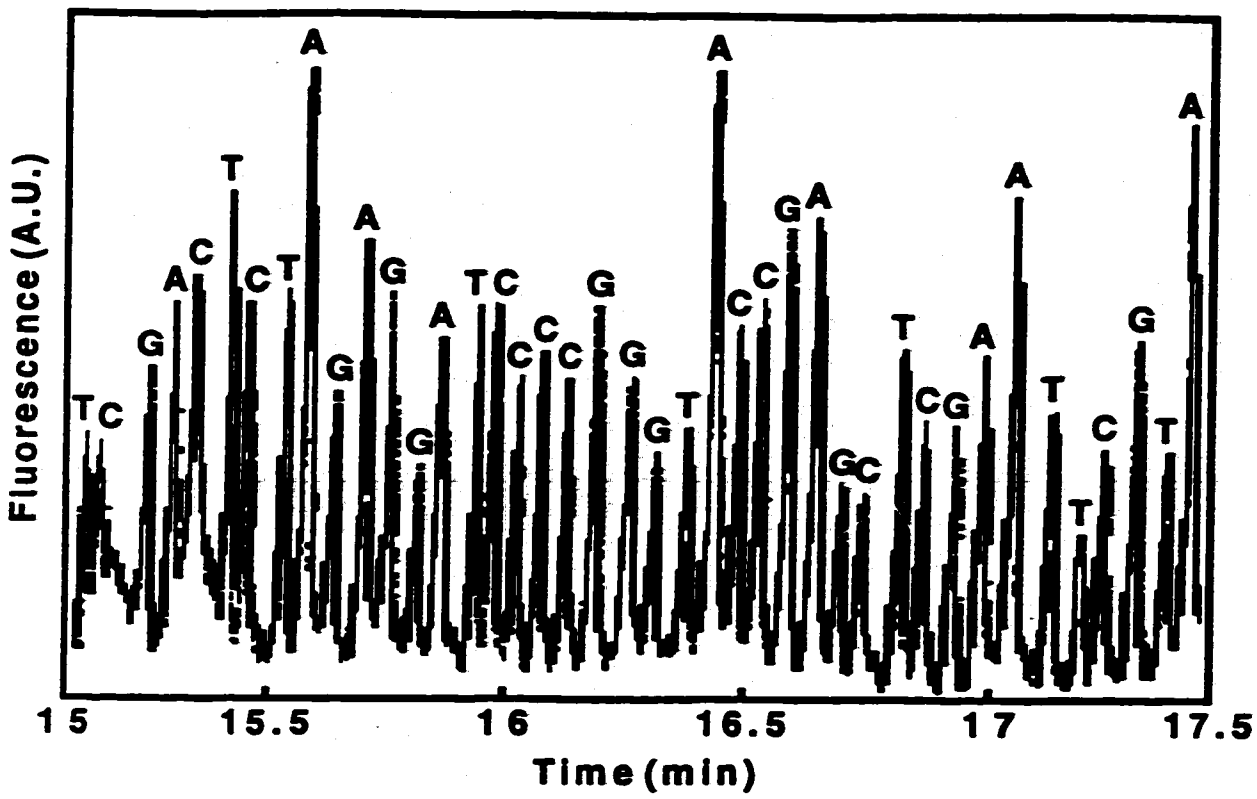

Figure 1.5: Two-spectral-channel-sequencing electropherogram of M3mp18 detailing nucleotides 60-100 with the known sequence labeled above each peak. Adapted from [23].

In practice longitudinal diffusion is not the only source of analyte dispersion. Dispersion contributions from Joule heating, interactions between the analyte and the capillary wall, electrodispersion, the sample injection, the detector, and siphoning due to unleveled capillary ends, must all be taken into account.

$$\sigma^2_{tot} = \sigma^2_{diffusion} + \sigma^2_{heating} + \sigma^2_{wall} + \sigma^2_{electrodispersion} + \sigma^2_{injection} + \sigma^2_{detector} + \sigma^2_{siphoning} \quad (1.7)$$

However, with careful control of the separation conditions many of these contributions may be reduced significantly, such that the major dispersion source is longitudinal. This is what allows CZE to have such high separation efficiencies. Therefore, assuming a longitudinal diffusion limited separation, the number of theoretical plates may be described by:

$$N = \frac{L_D^2}{\sigma_{tot}^2} \tag{1.8}$$

For on-column detection, substituting equation 1.6 into 1.8 gives:

$$N = \frac{L_D \mu_T V}{2 D L_T} \tag{1.9}$$

Interestingly, if end-column detection is used, equation 1.9 reduces to:

$$N = \frac{\mu_T V}{2 D} \tag{1.10}$$

where the number of theoretical plates achieved is no longer dependent on the length of the capillary.

In both cases, it is desirable to use a high separation voltage, analytes with small diffusion coefficients and electrolytes that result in a high EOF, as this will increase μ_T.

1.2 Detection

The silica capillaries used most often for CE separations are optically transparent to both UV (>200 nm) and visible light. This permits them to be used for on-column optically based detection schemes without the need for a separate detection cell. This is of value as it eliminates the presence of joints or connectors between the separation capillary and the detection cell which can introduce additional sources of dispersion into the separation.

Many of the detection schemes that are used in CE today have been adapted from HPLC. Thus a variety of on- and end-column detectors are available for use. Detector technology for CE often requires special adaptations to be made to the detector to accommodate either the capillary (typically 150-400μm outer diameter, o.d.), the electric field used for the separation, or the running electrolyte. In many cases these modifications are minor and detector modification is not a serious limitation. However, some detection schemes, e.g. mass spectrometry, require extensive modifications either to the capillary or to the interface between the separation capillary and the detector itself.

1.2.1 Detection Constraints

If a hypothetical separation is assumed whereby a detected solute exhibits a separation efficiency of *ca.* 500,000 theoretical plates and has a migration time of 5 min in a 40cm long (to the detector) capillary, an estimation of the solute width, in time, may be calculated by employing equation 1.11:

$$w_b = \frac{t_m}{\left(\frac{N}{16}\right)^{1/2}} \qquad (1.11)$$

where w_b is the width at the base of the detected solute peak (in time), t_m is the migration time of the solute and N is the number of theoretical plates.

The length of the detected solute zone in the capillary may now be determined from w_b by first recognizing that this length corresponds to 4 σ for a Gaussian peak which in turn represents 95% of the total peak width. Thus, by employing a corrected peak width representing 100% of the width of the peak and the migration velocity of the solute, the length of the detected solute zone may be calculated. For the above example the calculated zone width is *ca.* 2mm.

Generally, it is desirable to have the detector viewing region set to 10% of the width of the narrowest zones expected [24] in order to avoid the introduction of any zone broadening on the analytes from the detector. This would correspond to a detector viewing region of 200μm. Given that the capillary (in this example) has an i.d. of 50μm, this corresponds to a detection volume of only 500pL.

In addition, the available optical path length is even smaller than the internal diameter of the capillary since the capillary is in the shape of a cylinder. The available path length may be calculated using equation 1.12 [24]:

$$b = \frac{\pi \cdot \text{i.d.}}{4} \qquad (1.12)$$

where b = available path length.

Thus a 50μm i.d. capillary has an available optical path length of only *ca.* 39μm. This is more than 100 times smaller than that available with conventional HPLC

detectors. It is evident that any detector that is used must be able to cope with very small detection volumes.

This is not the only problem faced with regard to detection in CE. The dynamic range of the technique is constricted not only by the limit of detection (LOD), but by the highest acceptable analyte concentration for an analysis. In order to prevent electrodispersion and achieve reproducible symmetric peaks, the analyte concentration must be kept at least 100 times lower than that of the running electrolyte [25]. Therefore, some detection schemes may only be useful over 2-3 orders of magnitude. In such situations, the only way to increase the available dynamic range is to lower the LOD.

Finally, as biotechnology continues to expand, increasingly smaller substance amounts and concentrations are required to be quantitated. CE, due to its inherent ability to provide highly efficient separations [26] with microsampling capability [27], is attractive for the routine analysis of biological samples. However, improved detection strategies are necessary to provide the detection limits and sensitivities required for such analyses.

1.2.2 Detection Schemes

Table 1.1 details the current detection methodologies and their approximate detection limits when used with CE. As stated previously, all optical detection methods have the advantage of being able to be performed on-column, without end capillary detection cells requiring specialized joints or connectors. However, despite these advantages, it is clear from Table 1.1, that virtually all of the optical detection schemes have the highest LOD's, relative to end column detection methods.

Detector	Approximate Detection Limits	
	Moles	Molarity*
UV-Vis Absorbance	10^{-13} - 10^{-16}	10^{-5} - 10^{-7}
Indirect Absorbance	10^{-12} - 10^{-15}	10^{-4} - 10^{-6}
Fluorescence	10^{-15} - 10^{-17}	10^{-7} - 10^{-9}
Indirect Fluorescence	10^{-14} - 10^{-16}	10^{-6} - 10^{-8}
Laser-Induced Fluorescence	10^{-18} - 10^{-20}	10^{-9}-10^{-12}†
Mass Spectrometry	10^{-16} - 10^{-17}	10^{-8} - 10^{-10}
Amperometric	10^{-18} - 10^{-19}	10^{-7} - 10^{-10}
Conductivity	10^{-15} - 10^{-16}	10^{-7} - 10^{-9}
Refractive Index	10^{-14} - 10^{-16}	10^{-6} - 10^{-8}
Radiometric	10^{-17} - 10^{-19}	10^{-10} - 10^{-12}

*Dependent upon volume of sample injected.

Table 1.1: Capillary electrophoresis detectors and approximate detection limits. Reproduced from [28] except † [29].

End-column detectors, while being sensitive, often have additional considerations when used for CE separations. For example, in order to employ CE with electrospray-ionization mass spectrometry (ESI-MS) detection, the incoming buffer (and analytes) require dilution with a volatile liquid, such that effective spraying into the instrument may be achieved [30] The reason for this type of setup is twofold: (1) depending on the separation conditions, the CE flow rate may not be large enough to provide stable ESI, and (2) run buffers with ionic strengths above 0.01 M are not effectively electrosprayed [28]. An alternative is to use specialized buffers that are volatile enough to be effectively electrosprayed [31]. However, the number of buffers available is restricted.

For CE separations electrochemical detection methods necessitate isolation of the electric field used for the CE separation from the detector, or the use of a small i.d. capillary (*ca.* 5μm) to be used for the separation. These are necessary as high noise levels result when the detectors are exposed to the electrophoresis electric field. The first procedure requires a detection cell or capillary to be attached to the end of the separation capillary, while the latter method results in a low current flow through the separation capillary which does not interfere with the detector.

Thus, despite their excellent LOD's, end-column detection methods are not as simple to perform as on-column detection schemes. However, there is one optical detection method listed in Table 1.1 that has LOD values lower than any of the other optical detection schemes listed. Laser-induced fluorescence (LIF) is capable of providing very low detection limits [32,33], even to the single molecule level [34].

1.2.3 Laser-Induced Fluorescence Detection

For dilute solutions, fluorescence intensity is directly proportional to the power of the excitation radiation. This is illustrated in equation 1.13 [35]:

$$\Phi_F = 2.3\ \phi_p\, \varepsilon\, c\, l\, P \qquad (1.13)$$

where Φ_F is the fluorescence radiant intensity in W, ϕ_p is the quantum yield of fluorescence, ε is the molar absorptivity at the excitation wavelength in L / (mol · cm), c is the concentration of the analyte in mol/L, l is the optical path length in cm, and P is the radiant power of the excitation source in W.

It is clear from equation 1.13 that doubling the power of the excitation radiation will result in a like increase in the power of the emitted fluorescence. However, as stated above this is only valid for dilution solutions. Once the sample concentration increases to the point where the absorbance is greater than *ca.* 0.05, the linearity of a fluorescence intensity versus concentration plot is lost (for a 1cm path length) [36]. This occurs for two main reasons, self-quenching and self-absorption. Self-quenching occurs when a fluorescent molecule absorbs energy through a radiationless process from a neighboring excited fluorescent molecule which is eventually dissipated as heat. Self-absorption results when the emitted fluorescence has a wavelength which corresponds to an absorption wavelength for the fluorophore. The observed fluorescence is decreased by the amount of absorption by other fluorophores.

As a result of the dependence of equation 1.13 on the power of the excitation source, path length constraints on signal intensity are much less severe in fluorescence relative to absorbance detection. This has important implications for CE, where optical path lengths are on the order of μm. Therefore, improvement of detection limits in CE for a given fluorophore may be facilitated by employing an excitation source with a higher power output. For this reason, lasers are particularly attractive for fluorescence detection.

It is important to note that the output power of the excitation source cannot be increased arbitrarily. A point is reached where saturation of the fluorescence process occurs and further increases in excitation power do not result in increased fluorescence output [37]. This is illustrated by equation 1.14:

$$\Phi_F = \Phi_{F,max} \cdot \frac{E}{E + E_s} \qquad (1.14)$$

where $\Phi_{F,max}$ is the radiant intensity of fluorescence and, E is the irradiance of the source and E_s is the fluorescence saturation irradiance.

Once E becomes equal or larger than E_s, the fluorescence process becomes saturated and Φ_F will reach $\Phi_{F,max}$. Equation 1.13 is now no longer valid and further increases in the excitation power will not result in fluorescence gains. This typically occurs when the excitation source is a laser as in LIF.

The excitation power raises an additional concern with regard to the photostability of the fluorophore. If the excitation intensity is too high, destruction of the excited fluorophore may occur. This process is termed photobleaching as it results in reduced overall fluorescence emission. The easiest way to avoid this problem is to ensure that the fluorescence instrument is adjusted to provide the highest possible detection sensitivity and to use an excitation power that will provide the maximum possible fluorescence without resulting in photobleaching of the fluorophore.

A generic on-column LIF detection system is detailed in Figure 1.6. Laser light is focused by means of a focusing objective onto a section of the capillary where the polyimide coating has been removed. The excitation light is focused to a spot having a radius comparable to, or smaller than, the i.d. of the capillary. The emitted fluorescence is collected at 90^o to the excitation source and is passed through a collection objective and one or more wavelength selection filters.

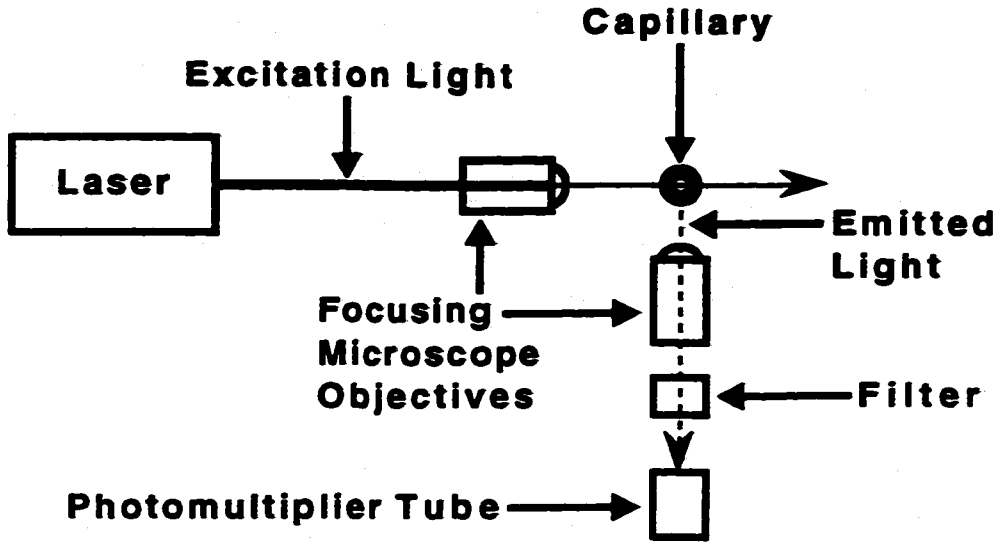

Figure 1.6: Generic design of a CE-LIF detector.

The purpose of the optical filter(s) is to eliminate fluorescence from the capillary, and Raman and Rayleigh scatter. The majority of the observed Raman scatter is caused by interactions between the laser light and the electrolyte solvent. The resulting scattered radiation has longer wavelengths than the excitation source. Rayleigh scatter is a form of elastic scatter that is caused predominately by interactions between the laser light and the capillary wall-electrolyte interfaces.

When compared with conventional light sources, laser light possesses some inherent advantages: laser light is coherent, meaning that each photon of light produced in the laser is in phase with all other emitted photons; the emitted light is monochromatic; and the emitted light beam is highly directional. This last criterion, in conjunction with the coherence of the light, allows focusing of the light beam into a radius comparable in

size to the wavelength [38]. Thus, focusing laser light into a spot the size of the i.d. of a CE separation capillary may be easily achieved.

All of these qualities provide lower LOD's with LIF detection as compared to conventional fluorescence detection. In addition, due to the monochromaticity of the excitation source, detection will be selective as only fluorescence from the analytes of interest will be detected. However, despite the lower LOD's and the inherent selectivity, there are disadvantages to employing LIF detection: (1) when employing a laser for excitation, the narrow wavelength emission significantly limits the number of fluorophores that may be used; therefore (2) the choice of laser becomes extremely important in order to select the wavelength that is the most versatile for the application of interest, and (3) most molecules are not naturally fluorescent and must undergo chemical reactions or be derivatized with a fluorescent probe to produce a fluorescent molecule.

1.3 Fluorescent Labeling of Biomolecules

Many proteins and peptides exhibit native fluorescence due to the presence of the aromatic amino acid residues phenylalanine (Phe), tyrosine (Tyr) and tryptophan (Trp). Each of one of these amino acids absorb and fluoresce in the UV region of the electromagnetic spectrum [39]. Trp is the most fluorescent of the three, however, each of these amino acids fluoresce only weakly and possess fluorescent quantum yields of 0.21 or less [40]. Phe fluoresces so weakly that it is not normally useful in a fluorescence analysis. In addition, their observed fluorescence is dependent on their local environment within the protein or peptide [41] and it is also possible that these amino acids may not be present in the biomolecule of interest. For example, a study of over 200 proteins has

shown that Tyr occurs with an average frequency of *ca.* 3.5% in proteins, while Trp occurs with an average fequency of only *ca.* 1.1% [42].

Thus, native fluorescence will not be a universal mode of detection for small biomolecules such as peptides. In addition, in order to use LIF, UV lasers must be used in order to provide the appropriate excitation wavelengths. Due to the relative cost of UV lasers as compared to visible wavelength lasers (e.g. He-Ne or Ar^+ ion lasers), much of the LIF work to date has focused on methods to introduce fluorescence by means of conjugation with a highly fluorescent tag [43-45], such that excitation may be facilitated with an inexpensive visible wavelength laser.

Performing the LIF detection of fluorophore conjugated analytes not only allows for an inexpensive instrument design, but its selectivity can be utilized for complex sample analysis [46] since only those analytes that are labeled with a fluorescent tag will be detected, simplifying the analysis procedure. Lower limits of detection are usually possible as the fluorescent tags employed are selected not only for their conjugating abilities, but also for their fluorescence properties [47].

Unfortunately, problems do exist with analyte derivatizations. The most significant common hindrance is the presence of more than one reactive site on the analyte of interest. This can result in multiple tagging with more than one label attached to the analyte. Usually, a distribution of labels is obtained [48] making any type of quantitative analysis difficult or impossible to perform. This is particularly true for large peptides or proteins. An example of this is shown in Figure 1.7.

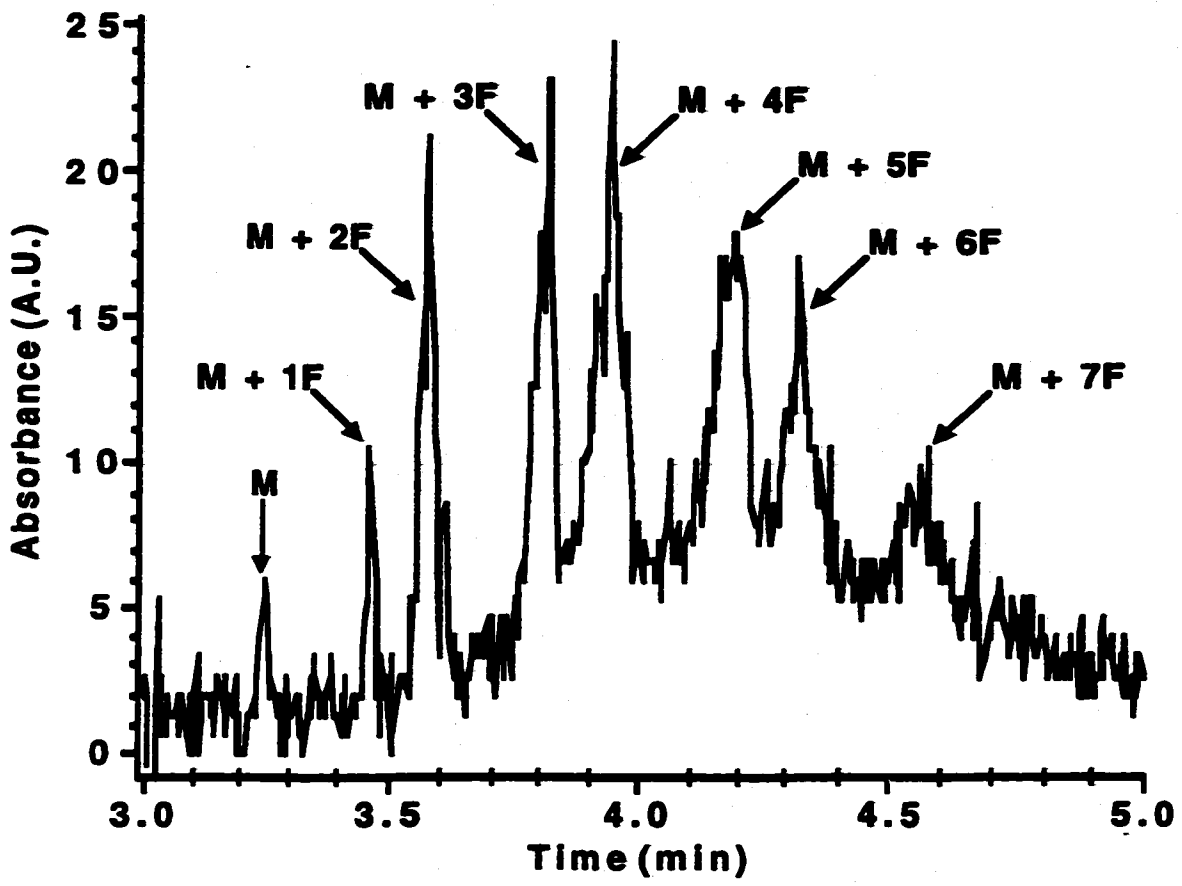

Figure 1.7: Electropherogram for a 10:1 molar ratio conjugation of fluorescein isothiocyanate (F) to myoglobin (M) which has been stopped by the addition of hydroxylamine after 1 hr and the conjugation mixture passed through a G-25 column. Peak assignments denote the number of fluorescent tags attached to myoglobin. Adapted from [48].

An additional problem is that complete derivatization of the analyte does not generally occur as the fluorescent tags that are used are quite bulky resulting in steric hindrances that can prevent additional tag attachment [48]. Therefore, quantitation becomes virtually impossible as the number and location of tags on each molecule of the analyte is not consistent. Attempts to separate the derivatization mixture generally

results in complex or indecipherable electropherograms [49]. An example of this is illustrated in Figure 1.8.

Currently, there are several different labeling/detection methods available as a means to introduce fluorescence to a non-fluorescent analyte. These are discussed in Section 1.3.1

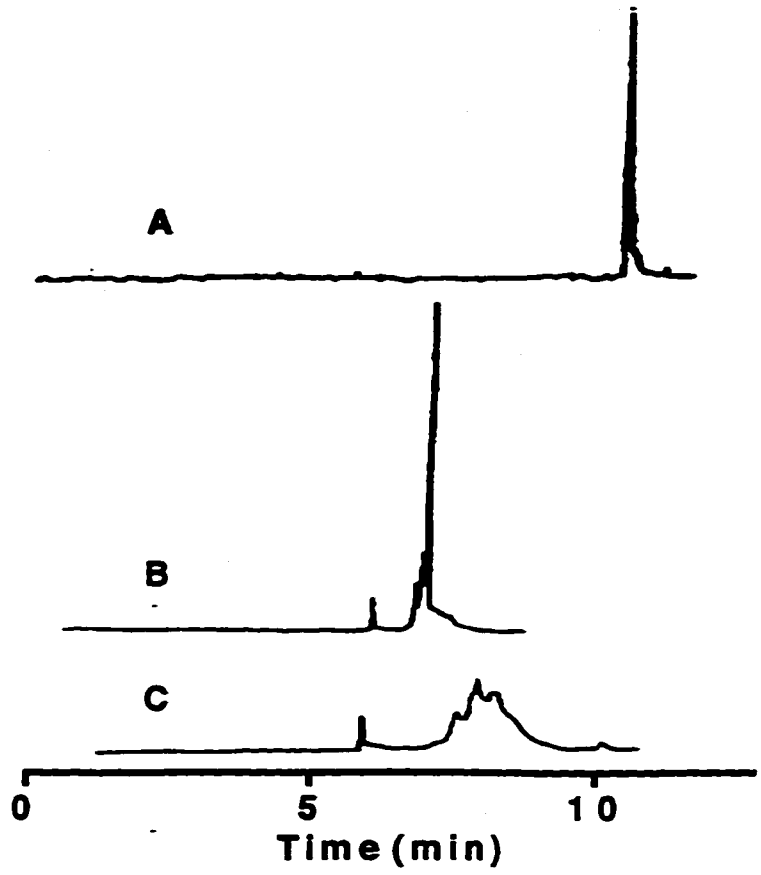

Figure 1.8: (A) Native fluorescence of conalbumin; (B) A 5:1 Fluorescein isothiocyanate / conalbumin derivatization; (C) A 10:1 Derivatization. Adapted from [47].

1.3.1 Labeling / Detection Methods

There are four common methods for the production of a fluorescent compound from a non-fluorescent analyte. The first method is useful if the analyte of interest is an enzyme capable of producing a detectable change through consumption of a fluorescent substrate to produce a nonfluorescent product or vice versa. During the analysis, the enzyme is introduced into a CE capillary containing a suitable buffer with the necessary substrate(s) for the enzyme. The observed fluorescence signal may either decrease or increase as the product zone migrates through the detection zone of the capillary. Since 10^3-10^6 product molecules may be produced per enzyme molecule, 10^{-21} mol of enzyme may be detected [50]. Of course, the amount of amplification will be dependent on the experimental conditions of the separation (e.g. reaction time, temperature and migration velocity) and the turnover number of the enzyme.

Another method involves the use of immunoassays where a fluorescently tagged antigen is used in a competitive immunoassay to quantitate the amount of native unlabeled antigen in a sample. Koutny *et al.* used this method to quantitate serum cortisol [51] via CZE-LIF on a chip. This method is very useful provided that the analyte of interest may also act as an antigen in a competitive immunoassay. An advantage is that direct derivatization of the analyte (antigen) is not necessary. This is particularly important when analyzing complex samples, as the presence of additional derivatizable compounds may lead to indecipherable electropherograms.

A third method involves the use of hydrophobic probes that fluoresce when interacting with a biomolecule hydrophobically. These probes fluoresce significantly only in non polar solvents unless buried in a protein, where the effects of the polar solvent are not as influential. For example, a CE-LIF separation of conalbumin, bovine

serum albumin and ß-lactogloblin A derivatized with 2-p-toluidinonaphthalene-6-sulfonate provided femtomole level detection limits of the analytes [47].

The final method, and perhaps the most popular, involves covalent attachment of a fluorescent tag to the analyte of interest. Tags which produce light for quantification may be chemiluminescent or fluorescent. Chemiluminescent techniques are limited as there are few reactions which are capable of producing chemiluminesence. Even though background signals are very low, the LOD's are typically not as high as for fluorescence techniques since each chemiluminescent reaction produces only one photon, whereas most fluorophores can undergo several thousand excitation/emission cycles, each one producing a photon of light, before being destroyed by photobleaching [23]. Thus chemiluminescent techniques have not found wide spread use in CE.

Fluorescent tags may be of two types, fluorogenic or non-fluorogenic. Fluorogenic tags are only fluorescent upon conjugation with an analyte, whereas non-fluorogenic tags already possess an intrinsic fluorescence both before and after conjugation Fluorogenic tags aid in detection as the unreacted reagent does not have to be separated from any of the analytes of interest in order to allow complete quantitation of the conjugated analyte. Tags that are non-fluorogenic before analyte conjugation have the potential of complicating the separation analysis if they are not resolved from the analytes of interest.

Derivatizations may take place either pre-, post-, or on-capillary. Most derivatizations to date have been pre-capillary as they are the simplest to perform practically. Generally, large volumes of reactants are required at relatively high concentrations for most reactions [23]. Large volumes are used as a matter of practicality, as volume handling below the µL level is not trivial. High concentrations are required

relative to the detection limit of the system, usually μM or above, as most tagging reactions are slow and undergo competing side reactions such as hydrolysis.

Post-capillary derivatizations require a rapid reaction time with a reagent that has different spectroscopic properties when conjugated to the analyte [43]. Post-capillary derivatizations have several advantages. For example, the derivatization reaction does not have to go to completion and a fixed number of fluorophores does not have to be attached to the analyte. However, the derivatization procedure must be reproducible such that quantitative results may be obtained. Disadvantages of the technique are that the LOD's are usually lower than those obtained with pre-capillary derivatizations [43] and that the separation capillary must be connected to another capillary containing the fluorescent reagent. This is usually facilitated via a T-junction usually producing additional zone dispersion.

On-capillary derivatizations are probably the least common of the three derivatization techniques and typically involve two capillaries connected together for the purpose of introducing the tagging reagent and analyte. The labeling reaction occurs in the junction prior to separation [52]. On- and pre-capillary derivatizations have the disadvantage of modifying the analytes prior to separation from their sample matrix which may lead to complicated electropherograms through incomplete separation of multiply labeled products.

Currently, there are a number of fluorescent reagents available for covalent derivatization. They contain a wide range of reactive moieties that are capable of reacting with various analyte functional groups [53]. One of the most common fluorescent reagents and its derivatives are discussed in Chapter 1.3.2.

1.3.2 Fluorescein and its Derivatives

Fluorescein derivatives have a wide-spread popularity for the labeling of amino groups found on proteins [53-55] and other analytes [44]. There are several reasons for this including its low cost, its high absorptivity and quantum yield, as well as an excitation maximum (494 nm) that closely matches the 488 nm emission line of an Ar^+ laser. It is worth mentioning that in addition to the qualities listed above, fluorescein derivatives also have some drawbacks which include a high rate of photobleaching [56], pH sensitive fluorescence [57] and partially quenched fluorescence upon protein/peptide conjugation [58,59]. Aside from the latter drawback, each of these may be overcome through careful optimization of the experiment.

Fluorescein isothiocyanate (FITC), carboxyfluorescein succinimidyl ester (CFSE), and fluorescein dichlorotriazine (DTAF) are the three most common amine-reactive fluorescein derivatives. Their structures are shown in Figure 1.9. Of the three fluorescein derivatives, FITC is the most popular [53] and has been used for labeling proteins and peptides in a wide range of applications [60,61] while CFSE is the labeling reagent of choice for bioconjugate preparations by some [62].

Recently, each of these labeling reagents was studied to determine their rate of conjugation, extent of hydrolysis and bioconjugate stability [63]. CFSE exhibited the fastest conjugation rate, while FITC reacted *ca.* 15 times slower, displaying the lowest reaction rate of the three reagents. The rate of reagent hydrolysis was found to be generally insignificant at the pH studied when compared to the amine conjugation rates. Lastly, the CFSE bioconjugates were found to have the greatest stability over time, while the FITC bioconjugates had the lowest. However, a CZE analysis of the unreacted reagents showed that FITC displayed a single peak in the electropherogram, well resolved

from any of its hydrolysis products, whereas CFSE and DTAF each provided complex electropherograms which could lead to difficulties when quantitative analyses are required. In addition, as FITC displayed the slowest conjugation rate of the three, manipulation of the probe-analyte exposure time may be possible allowing a control over the number of labelled products produced during the reaction.

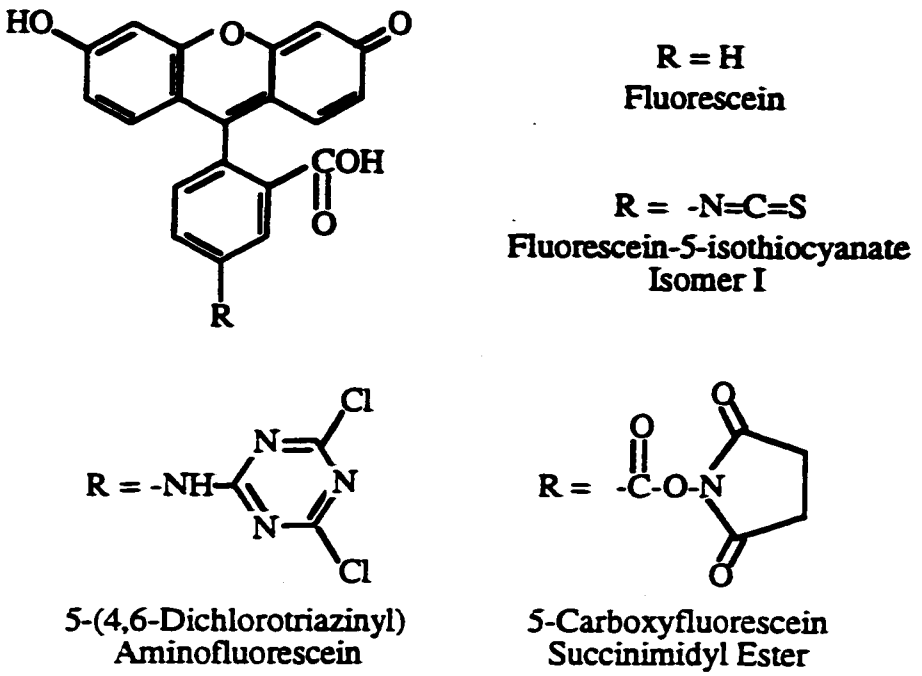

Figure 1.9: Structure of fluorescein and its amine reactive derivatives.

Another advantage of FITC is that the reactive moiety is an isothiocyanate group. This allows the reagent to be used in the Edman degradation procedure for the sequencing of proteins and peptides [64]. FITC has also been used in combination with phenylisothiocyanate to provide peptides with a single label [65].

1.4 Thesis Organization

The goal of the work described within this thesis was to determine if a single fluorescent label could be attached to a small peptide at its N-terminus with a high degree of selectivity. While a method is available to attach a single fluorescent label to a small peptide [65], the derivatization procedure is rather involved. A simple one-step derivatization under the appropriate experimental conditions would be a more attractive and useful method. This represents the goal of work presented herein.

Previous work in this laboratory [63] and others [66,67] has shown that FITC displays a selectivity for N-terminal amino groups over ε-amino groups present on lysine side chains in biomolecules. Chapter 2 of this thesis details our methodology for optimization of the N-terminal selectivity that FITC demonstrates. A kinetic study was carried out on the pH dependent reaction between FITC and α- or ε-BOC-L-lysine. The pH range studied was between 7.5 and 10 and the relative reaction rates of α-amino versus ε-amino conjugation were determined as a measure of the α-amino selectivity.

Chapter 3 continues the α-/ε-amino conjugation study through the derivatization of several small peptides to observe the extent of α-amino selectivity. This was a qualitative study to determine the number of derivatives produced from each peptide conjugation.

Chapter 4 is a summary of the results presented in Chapters 2 and 3, and presents suggestions for future work.

1.5 References

1. B. Tenberken and K. Bäckmann, *J. Chromatogr.*, 755 (1996) 121.

2. M. T. Combs, M. Ashraf-Khorassani and L. T. Taylor, *Anal. Chem.*, 68 (1996) 4507.

3. K. A. Koeplinger and Z. Zhao, *Anal. Biochem.*, 243 (1996) 66.

4. O. Mamam, F. Marseille, B. Guillet, J. R. Disnar and P. Morin, *J. Chromatogr.*, 755 (1996) 89.

5. D. Volgger, A. J. Zemann, G. K. Bonn and M. J. Antal, Jr., *J. Chromatogr.*, 758 (1997) 263.

6. S. Terabe, K. Otsuka and T. Ando, *Anal. Chem.*, 57 (1985) 834.

7. S. D. Gilman and A. G. Ewing, *Anal. Chem.*, 67 (1994) 58.

8. S. Hjertén, *Chromatogr. Rev.*, 9 (1967) 122.

9. F. E. P. Mikkers, F. M. Everaerts and Th. P. E. M. Verheggen, *J. Chromatogr.*, 169 (1979) 11.

10. J. W. Jorgenson and K. D. Lukacs, *J. Chromatogr.*, 218 (1981) 201.

11. J. W. Jorgenson and K. D. Lukacs, *Anal. Chem.*, 53 (1981) 1298.

12. T. Wehr and M. Zhu, *Handbook of Capillary Electrophoresis*, Landers, James P., Ed., CRC Press, Boca Raton, Florida, 1994, chap. 1.

13. J. W. Jorgenson and K. D. Lukacs, *Science*, 222 (1983) 226.

14. S. V. Ermakov, M. Y. Zhukov, L. Capelli and P. G. Righetti, *J. Chromatogr. A*, 699 (1995) 297.

15. M. R. Schure and A. M. Lenhoff, *Anal. Chem.*, 65 (1993) 3024.

16. B. L. De Backer and L. J. Nagels, *Anal. Chem.*, 68 (1996) 4441.

17. H. J. Tarigan, P. Neill, C. K. Kenmore and D. J. Bornhop, Anal. Chem., 68 (1996) 1762.

18. E. S. Yeung, *Adv. Chromatogr.*, 35 (1995) 1.

19. J. Cai and J. Henion, *J. Chromatogr. A*, 703 (1995) 667.

20. G. A. Parks, *Chem. Rev.*, (1965) 177.

21. R. M. McCormick, *Anal. Chem.*, 58 (1988) 2322.

22. M. F. M. Tavares and V. L. McGuffin, *Anal. Chem.*, 67 (1995) 3687.

23. H. Swerdlow, J. Z. Zhang, D. Y. Chen, H. R. Harke, R. Grey, S. Wu and N. J. Dovichi, *Anal. Chem.*, 63 (1991) 2835.

24. S. L. Pentoney, Jr. and J. V. Sweedler, *Handbook of Capillary Electrophoresis*, Landers, James P., Ed., CRC Press, Boca Raton, Florida, 1994, chap. 7.

25. Baker, Dale R., *Capillary Electrophoresis*, John Wiley & Sons, Toronto, Ontario, 1995, chap. 2.1.

26. D. N. Heiger, A. S. Cohen and B. L. Karger, *J. Chromatogr.*, 516 (1990) 33.

27. D. Sziele, O. Brueggemann, M. Doering, R. Freitag and K. Schuegerl, *J. Chromatogr. A*, 669 (1994) 254.

28. Dale R. Baker, *Capillary Electrophoresis*, John Wiley & Sons, Inc., Toronto, Ontario, 1995, chap. 4.3

29. R. G. Giese, W. Li, P. Wang and E. S. Yeung, J. Chromatogr., 608 (1992) 73.

30. R. D. Smith, C. J. Barinaga and H. R. Udseth, *Anal. Chem.*, 60 (1988) 1948.

31. A. J. Tomlinson, L. M. Benson and S. J. Naylor, *LC-GC* 12 (1994) 122.

32. A. J. G. Mank and E. S. Yeung, *J. Chromatogr. A*, 708 (1995) 309.

33. L. Hernandez, N. Joshi, P. Verdeguer and N. A. Guzman, *Chromatogr. Sci. Ser.*, 64 (1993) 605.

34. B. B. Haab and R. A. Mathies, *Anal. Chem.*, 67 (1995) 3253.

35. C. M. B. Van Den Beld and Hank Lingeman, *Luminescence Techniques in Chemical and Biochemical Analysis*, Edited by W. R. G. Baeyens, D. De Keukeleire and K. Korkidis, Marcel Dekker, Inc., New York, 1991, chap. 9, p. 246.

36. M. Kubista, R. Sjöback, S. Eriksson and B. Albinsson, *Analyst*, 119 (1994) 417.

37. N. J. Dovichi, J. C. Martin, J. H. Jett, M. Trkula and R. A. Keller, *Anal. Chem.*, 56 (1984) 348.

38. Andrews, David L., *Lasers in Chemistry, Second Edition*, Springer-Verlag Berlin - Heidelberg, 1990, chap. 1.6.2.

39. T. E. Creighton, Proteins: *Structures and Molecular Properties*, Second Edition, W. H. Freeman & Company, New York, 1993, chap. 1, p. 14

40. F. W. J. Teale and G. Weber, *J. Biochem.* 65 (1957) 476.

41. A. T. Timperman, K. E. Oldenburg and J. V. Sweedler, *Anal. Chem.*, 67 (1995) 3421.

42. M. H. Klapper, *Biochem. Biophys. Res. Commun.* 78 (1977) 1018.

43. M. E. Szulc and I. S. Krull, *J. Chromatogr. A*, 659 (1994) 231.

44. X. Páez, P. Rada, S. Tucci, N. Rodríguez and L. Hernández, *J. Chromatogr. A*, 735 (1996) 263.

45. M.Albin, R. Weinberger, E. Sapp and S. Moring, *Anal. Chem.*, 63 (1991) 417.

46. O. Orwar, H. A. Fishman, N. E. Ziv, R. H. Scheller and R. Zare, *Anal. Chem.*, 67 (1995) 4261.

47. D. F. Swaile and M. J. Sepaniak, *J. Liq. Chrom.*, 14, 5 (1991) 869

48 P. R. Banks and D. M. Paquette, *J. Chromatogr. A*, 693 (1995) 145.

49. J. Liu, Y. Z. Hsieh, D. Wiesler and M. Novotny, *Anal. Chem.*, 63 (1991) 408.

50. K. J. Miller, I. Leesong, J. Bao, F. E. Regnier and F. E. Lytle, *Anal. Chem.*, 65 (1993) 3267.

51. L. B. Koutny, D. Schmalzing, T. A. Taylor and M.Fuchs, *Anal. Chem.*, 68 (1996) 18.

52. S. L. Pentony Jr., X. Huang, D. Burgi and R. N. Zare, *Anal. Chem.*, 60 (1988) 2625

53. R. P. Haugland, *Handbook of Fluorescent Probes and Research Chemicals*, M. T. Z. Spence, Ed.) Molecular Probes Inc., Eugene, OR, 5th Edition, 1996.

54. O. W. Reif, R. Lausch, T. Scheper and R. Freitlag, *Anal. Chem.*, 66 (1994) 4027.

55. H. Kawauchi, K. Tuzimura, H. Maeda and N. Ishida, *J. Biochem.*, 66, 6 (1989) 783.

56. L. Song, E. J. Hennik, I. T. Young and H. J. Tanke, *Biophys. J.*, 68 (1995) 2588.

57. R. Sjöback, J. Nygren and M. Kubista, *Spectrochim. Acta. A*, 51 (1995) L7.

58. G. P. Der-Balian, N. Kameda and G. L. Rowley, *Anal. Biochem.*, 173 (1988) 59.

59. R. F. Zuk, G. L. Rowey and E. F. Ullman, *Clin. Chem.*, 25 (1979) 1554.

60. K. Muramoto, K. Nokihara, A. Ueda and H. Kamiya, *Biosci. Biotech. Biochem.*, 58 (1994) 300.

61. S Wu and N. J. Dovichi, *J. Chromatogr.*, 480 (1989) 141.

62. Molecular Probes, Inc., Eugene, OR.

63. P. R. Banks and D. M. Paquette, *Bioconjugate Chem.*, 6 (1995) 447.

64. K. Muramoto, H. Kamiya and H. Kawauchi, *Anal. Biochem.*, 141 (1984) 446.

65. J. Y. Zhao, K. C. Waldron, J. Miller, J. Z. Zhang, H. Harkes and N. Dovichi, *J. Chromatogr.*, 608 (1992) 239.

66. H. Maeda, N. Ishida, H. Kawauchi and K. Tuzimura, *J. Biochem.*, 65 (1969) 777-783

67. W. W. Bromer, S. K. Sheehan, A. W. Berns and E. R. Arquilla, *Biochem.*, 6 (1967) 2378.

CHAPTER 2

FLUORESCENCE DERIVATIZATION - KINETIC STUDY

2.1 Introduction

When attaching a fluorescent tag to an analyte, the most common problem lies in the fact that more than one derivatizable site is present. When the analyte of interest is a protein or peptide this is most certainly the case. The result is multiple labeling, complex electropherograms and quantitation problems.

An ideal derivatization method would allow for the addition of a single tag to the analyte of interest. Dovichi *et al.* [1] employed Edman degradation chemistry to attach a single fluorescent label to a heptapeptide. The procedure involved taking the peptide through one cycle of the Edman degradation reaction. This resulted in the derivatization of all available amino groups with phenyl isothiocyanate (PITC), and the loss of the N-terminal amino acid from the peptide, exposing a new N-terminal amino group on the next amino acid in the peptide which was then reacted with FITC. The result was a singly labeled peptide.

While this procedure was able to demonstrate single labeling it is not necessarily an ideal choice. For example, as pointed out by the authors, due to the removal of the N-terminal amino acid, the differentiation of peptides which differed initially only at the N-terminal amino acid would not be possible. An additional drawback is the extensive modification of the analyte. Such modification would likely prevent further use of the analyte in biochemical studies, e.g. immunoassays.

A more facile method would be to use a one-step derivatization to attach a single label while producing a limited or negligible amount of multiply tagged analytes. The fluorescent label Dovichi used, FITC, has been shown by other groups to possess some chemical selectivity for the α-amino groups present on neocarzinostatin [2] and insulin [2,3]. Recent work by Banks and Paquette has shown that FITC conjugates with some selectivity to the α-amino group of lysine over the ε-amino group [4]. This is illustrated in Figure 2.1.

The principal reason for the selectivity resides in the reaction mechanism which is described as the nucleophilic attack of an uncharged primary amino group on the isothiocyanate carbon to produce a thiocarbamoyl derivative. The net reaction is illustrated in Figure 2.2. As a result, the pK_a and nucleophilicity of the amino group of interest are pertinent for an efficient reaction. In general, the pK_a values of the α-amino groups of the majority of the 20 naturally occurring amino acids are at least 0.8 pH units less than the pK_a of the ε-amino group of lysine. An exception is proline which has a pK_a value 0.4 pH units higher [5]. The explanation for this observation comes from the presence of an electron withdrawing carbonyl group one carbon away from the α-amino group. This causes the α-amino group to be less nucleophilic, and less basic, than other aliphatic amines such as lysine's ε-amino group. Proline is an exception as its α-amino group is a secondary amine resulting in a higher than average pK_a.

Therefore, the observed selectivity in Figure 2.1 is a result of the presence of a larger amount of uncharged, albeit less nucleophilic, α-amino groups compared to ε-amino groups at the pH of the conjugation reaction. At pH 9.28 *ca.* 36% of the α-amino groups are deprotonated and able to act as nucleophiles whereas only *ca.* 5% of the ε-amino groups are able to participate.

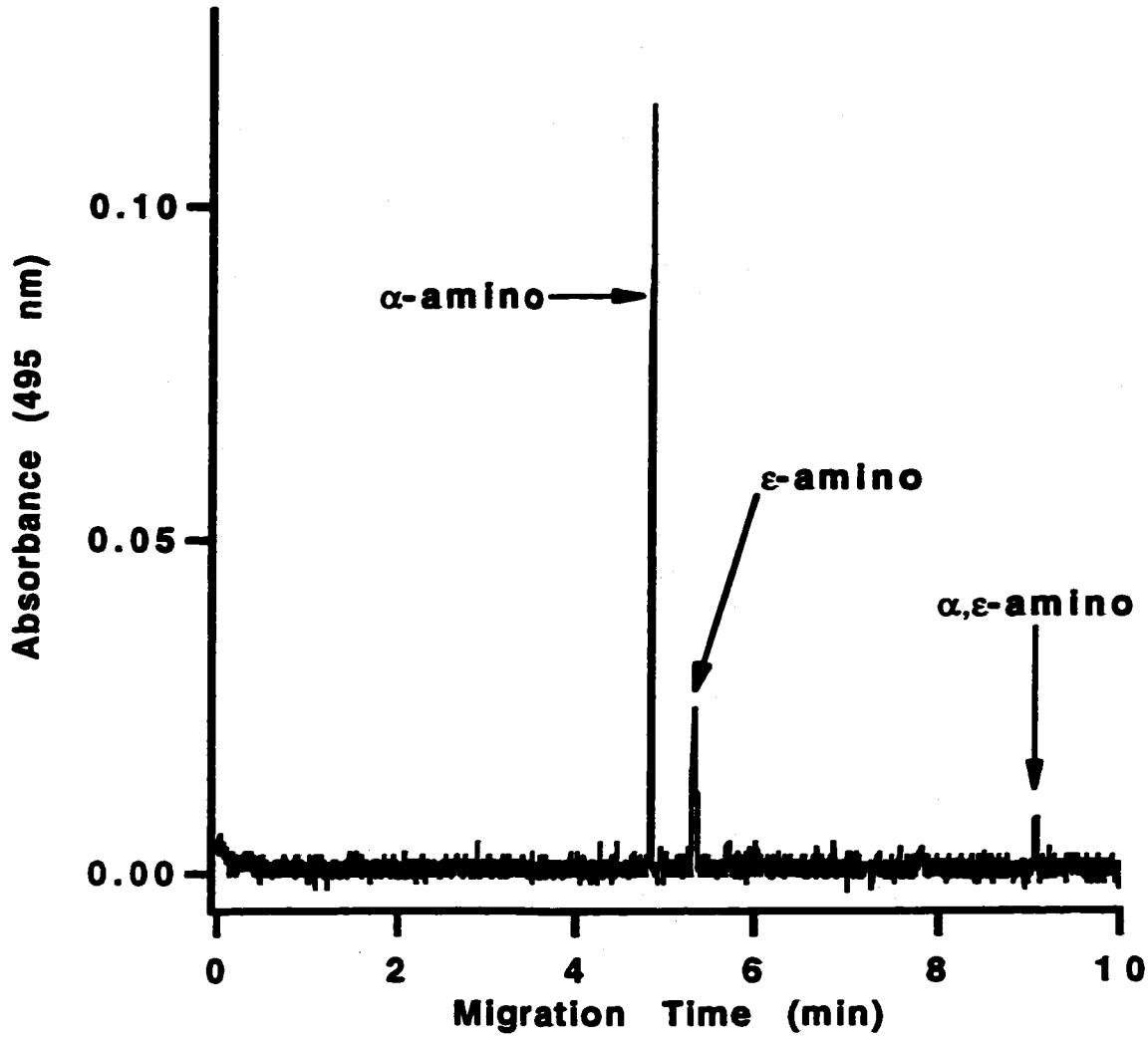

Figure 2.1: Electropherogram of a 5:1 reaction between L-lysine and FITC at pH 9.28. Adapted from [4].

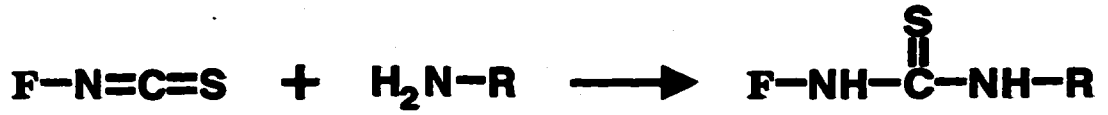

Figure 2.2: Net reaction of FITC coupling to a primary amine, where **F** denotes the fluorescein group.

Thus, the conjugation buffer pH plays a decisive role in the amount of observed α-amino selectivity. For an amino group of interest the fraction present in the uncharged form, θ, relative to the total amount present may be calculated at any pH based on Equation 2.1.

$$\theta = \frac{[RNH_2]}{[RNH_2] + [RNH_3^+]} = \frac{1}{10^{pKa-pH} + 1} \qquad (2.1)$$

Lysine's α-amino group has a pK_a of 8.95, while its ε-amino group has a pK_a of 10.53 [5]. If θ is evaluated for the α-amino (θ_α) and ε-amino (θ_ε) groups of lysine and the two results divided ($\theta_\alpha / \theta_\varepsilon$), the relative amount of uncharged α-amino to ε-amino groups may be obtained. This is illustrated in Figure 2.3 over a pH range of 7-11. Figure 2.3 may be used to obtain only a preliminary estimation of how the α-amino selectivity of the FITC derivatization reaction will be effected by the conjugation buffer pH as contributions from the relative nucleophilicities of each amino group are not taken into consideration with such a plot. Nevertheless, it appears as though by simply lowering the conjugation buffer pH, large increases in α-amino selectivity may be gained. Of interest is that most FITC conjugations are typically carried out in the pH range of 9.0-

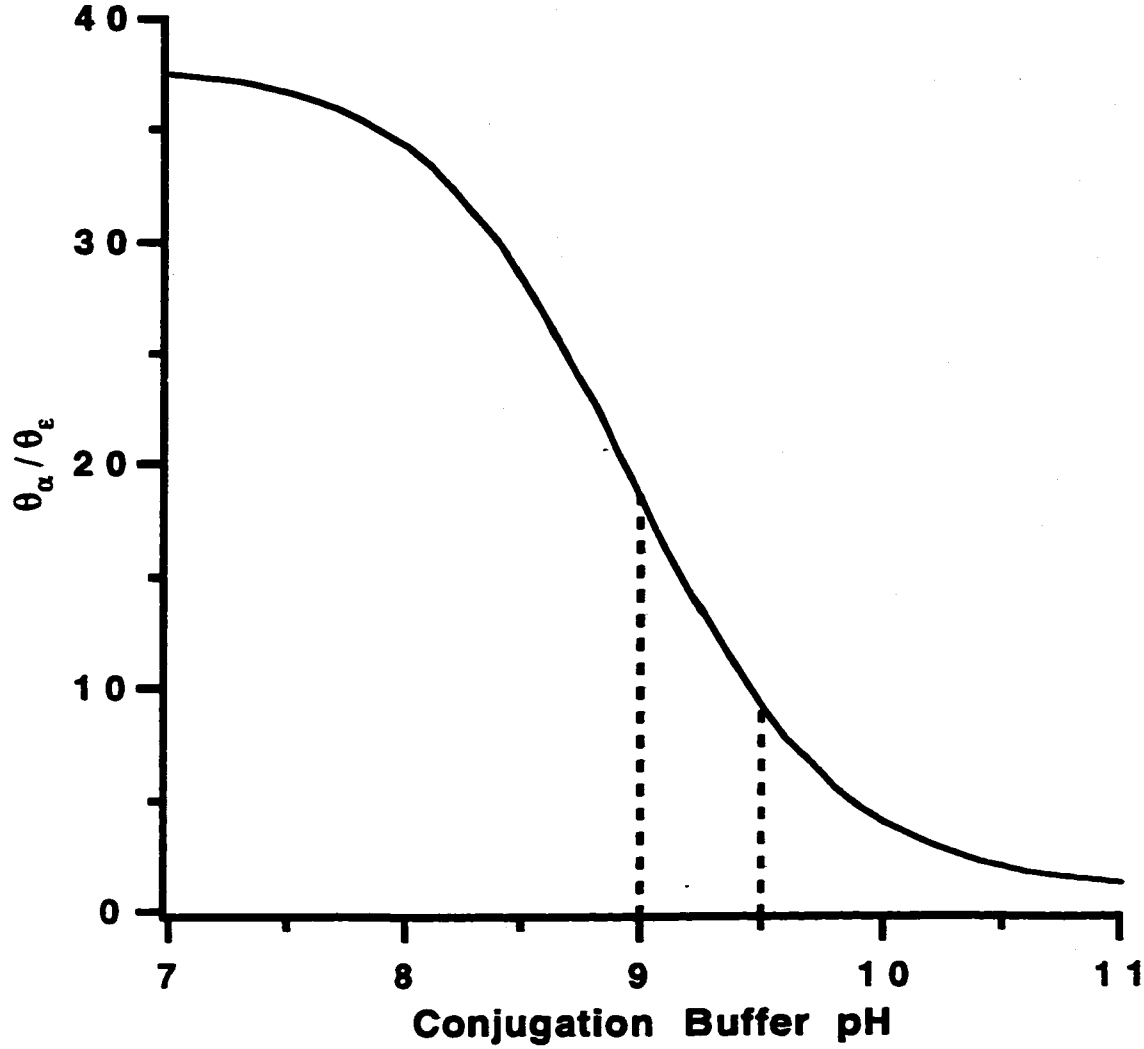

Figure 2.3: Calculated $\theta_\alpha / \theta_\varepsilon$ plotted as a function of conjugation buffer pH. The dashed vertical lines bound the typical pH range employed for biomolecule derivatizations by FITC.

9.5 [2,3,6] in order to produce the most efficient conjugation. These may not be the most effective pH's to produce a single or unique conjugate.

This study attempts to determine whether the α-amino group of a peptide may be selectively derivatized via control of the conjugation buffer pH and the molar ratio of the analyte and the derivatizing agent, FITC. If possible this method would be of practical use for CE-LIF determinations of biomolecules.

2.2 Experimental

2.2.1 Apparatus

All electrophoretic separations were carried out on an ATI-Unicam (Mississauga, Ont.) Model Crystal 310 CE system with a 48-position peltier-cooled auto sampler. Analytes were introduced into the separation capillary via dynamic compression of 20 mBar for 0.1 min. The sample tray in the Crystal 310 system could be temperature controlled in the range of 8-40 °C with ±1 °C stability. Derivatization reactions were contained in 250μL glass vials sealed with StarBurst™ caps to prevent evaporation while facilitating periodic sampling by the Crystal 310 system. The detector was a Unicam (Mississauga, ON) Model 4225 UV-absorbance detector equipped with a $^2H_2$ lamp operating at 200 nm. Fused-silica capillaries were obtained from Polymicro Technologies (Phoenix, AZ) and had an i.d. of 50μm and an o.d. of 350μm.

Voltages proportional to the absorbance signals were collected at 10 Hz with a National Instruments (Austin, TX) NB-MIO-16X-H, 16 bit resolution, data acquisition board and stored as binary files on a Power Macintosh (Apple, Cupertino, CA) Model 7100/66 using an application developed in the National Instruments (Austin, TX)

graphical programming language, LabView 3.1. The binary files were analysed with the WaveMetrics (Lake Oswego, OR) application Igor Pro.

2.2.2 Chemicals

Nα-t-BOC-L-lysine, Nε-t-BOC-L-lysine, Sigma grade borax, and Sigma ultra boric acid were obtained from Sigma (St. Louis, MO). HPLC grade N,N-dimethylformamide (DMF) and sodium hydroxide were obtained from Aldrich (Milwaukee, WI). Fluorescein isothiocyanate (FITC) Isomer I were obtained from Molecular Probes (Eugene, OR). HPLC grade water was provided by a neighboring laboratory with a Barnstead (Dubuque, Iowa) Nanopure system (specific resistance 18 MΩ · cm).

2.2.3 Methodology

A 20-fold excess of either Nα-t-BOC-L-lysine or Nε-t-BOC-L-lysine was used relative to FITC to allow for the measurement of the rate of reaction of FITC with either the α-amino group of Nε-t-BOC-L-lysine or the ε-amino group of Nα-t-BOC-L-lysine.

Derivatization conditions were as follows. The appropriate amine reagent was dissolved in 0.1 M borate buffer of the appropriate pH and a 200μL aliquot of the resulting solution was added to a 250μL glass vial designed to fit the CZE autosampler. Derivatization was initiated by the addition of a 2.32μL aliquot of an 86mM FITC solution in DMF to the glass vial. After addition of the FITC solution the timing of the derivatization reaction was begun and the reactants were thoroughly mixed with a disposable pipette. The glass vial was then inserted into the CZE autosampler and a preprogrammed method of multiple samplings and separation of the derivatization reaction products was initiated. All derivatizations were performed at 20 ± 1 °C.

The rate of reaction between the amine reagent and FITC was monitored by periodic separations of the reaction mixture by on-line CE. A small window was burned in the polyimide coating of the capillary *ca.* 10 cm from the grounded outlet buffer reservoir. New capillaries were treated before use by flushing them with 0.1 M of either KOH or NaOH for *ca.* 5min, followed by 0.1M borate run buffer of the appropriate pH, for a similar duration. The run buffer was then electrophoresed through the separation capillary for a period of *ca.* 30min as a final equilibration step prior to use. At the end of the day, the separation capillary was stored in run buffer overnight. Prior to re-use, the capillary was re-treated with run buffer as stated above.

Each separation procedure was identical with the exception of the electrophoretic separation time which was varied as necessary (2.75-8min) to detect of all analytes. The separation methodology was preprogrammed into the Crystal 310 system and consisted of five steps. Initially, the outside of the capillary and the electrode were rinsed by immersion into a vial of run buffer for 0.01 min. The sample was then injected as stated above, followed by another rinse of the capillary and electrode in the run buffer vial. The capillary and electrode were then immersed into a new vial of run buffer and electrophoresis was carried out. Separations were initiated via the application of either a 20kV (pH 10) or 22kV (below pH 10) positive potential to the inlet buffer vial through a Pt-Ir (80/20) wire. Current flow in the capillary varied between *ca.* 2 and 65μA depending on the pH of the run buffer. After the analysis, the capillary was flushed with run buffer using a pressure of 2300mBar for 0.5min.

FITC peak area versus time was measured using PeakBoy (Appendix I), an in-house developed peak integration Igor Pro macro. To establish the peaks attributable to the derivatized products and to correct for reduction of FITC peak area by hydrolysis,

blank solutions containing an identical amount of FITC in each of the conjugation buffers were monitored. This permitted an evaluation of the observed pseudo-first order rate constant for FITC hydrolysis. Although the observed hydrolysis rate constants were evaluated over the pH range of interest with a minimum of four replicates for each pH of interest, the observed hydrolysis rate constants for pH's 9.0, 9.5 and 10.0 were acquired from a similar study performed by Fabian Zaccardo [7]. This data was used to represent FITC hydrolysis at those pH's as the data acquired with this study over that pH range was not consistent with that of a base catalyzed reaction. Observed pseudo-first order rate constants for the derivatization reactions were calculated from the slopes of plots of ln (peak area) versus derivatization time. . At each pH studied, at least four separate derivatization reactions were performed to obtain an average rate constant for that pH.

20mM solutions of Nα- and Nε-t-BOC-L-lysine were titrated with NaOH using an Accumet® Model 15 pH meter with an Accu-pHast™ combination electrode Model 13-620-296 (Fisher Scientific, Montreal, PQ).

2.3 Results and Discussion

Work carried out by Zahradník [8,9] with a series of 20 alkyl, allyl and aralkyl isothiocyanates elucidated that the reaction rate of an isothiocyanate with a primary amine reagent was directly proportional to the concentrations of both reagents. When an excess of the primary amine reagent was used, such that $[RNH_2] >> [R'ITC]$, pseudo first order kinetics were realized with respect to the isothiocyanate reagent. In addition, the amines were shown to react only in their free base, the concentration of which was dependent on the dissociation reaction that preceded the coupling reaction. Consequently, the reactivity of different amino compounds toward isothiocyanates has

been shown to be correlated with their basicity [9]; an increased amine basicity results in an increased reaction rate.

Satchell and Satchell [10] presented the following general rate expression for the spontaneous reaction of an isocyanate and a primary amine reagent in several solvent systems:

$$\frac{d[\text{product}]}{dt} = \{k_1[RNH_2] + k_2[RNH_2]^2 + k_3[RNH_2][\text{urea product}]\}\ [RNCO] \qquad (2.2)$$

where $[RNH_2]$ refers to the concentration of the amine in the free base form. For example, in a non-hydroxylic solvent, product formation requires the formation of a cyclic transition state that may be stabilized either by the amine reagent or the urea product. The solvent may also form a cyclic transition state provided it is amphiprotic, non-hydroxylic and incapable of hydrogen bonding. These transition states are illustrated in Figure 2.4.

The authors claim that provided an excess of the primary amine reagent is used, the autocatalytic term, $k_3[RNH_2][\text{urea product}]$, is negligible in the rate expression. In addition, the authors also state that as the hydrogen bonding capacity of the solvent increases, the ratio of $k_1[RNH_2]$ to $k_2[RNH_2]^2$ rises, reducing the importance of the latter term in the rate expression. Once the hydrogen bonding capacity has reached a sufficient level, the only transition state expected for the reaction is that shown in Figure 2.4a. Even in situations where an excess of the primary amine reagent is not present, provided the hydrogen bonding capacity of the solvent is large enough, the autocatalytic term should remain negligible as the concentration of the reaction product would be

inconsequential when compared to that of the solvent. The overall rate expression will then reduce to:

$$\frac{d[product]}{dt} = k[RNH_2]\,[RNCO] \qquad (2.3)$$

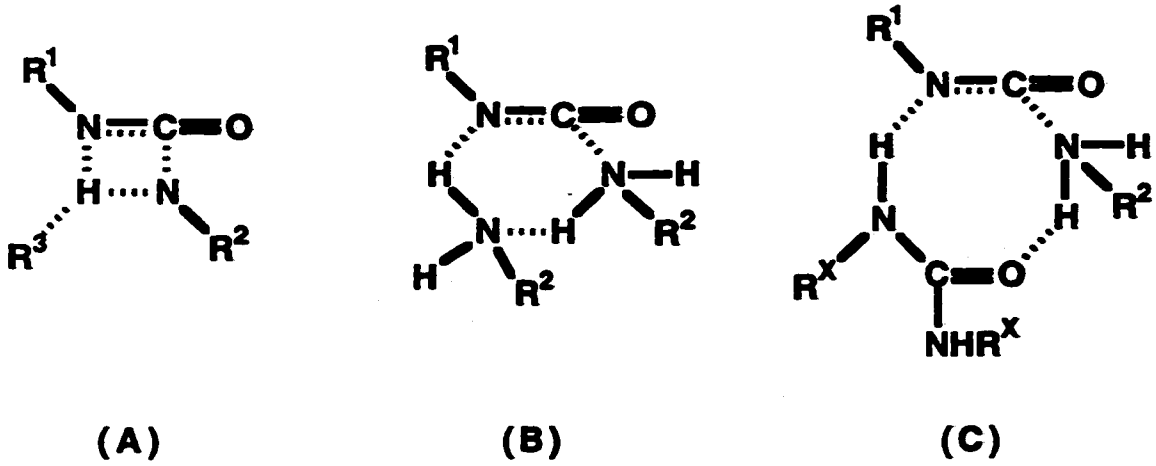

Figure 2.4: Possible cyclic transition states in the reaction of an isocyanate and a primary amine; stabilized by (a) the solvent, R^3, (b) the primary amine reagent, (c) the thiourea product. R^X may be either R^1 or R^2.

In an aqueous medium, the same transition state does not occur [10] as water is capable of extensive hydrogen bonding, has excellent amphiprotic properties, and its concentration would be enormous relative to any of the isocyanate-amine reaction species. Finally, the authors state that the reactions of an isothiocyanates with primary amine reagents undergo identical kinetic patterns to that of isocyanate - amine reactions. Therefore, the transition states similar to those presented in Figure 2.4 would also occur.

Egê detailed the coupling mechanism of PITC with a primary amine reagent as it occurs in the first step of the Edman degradation reaction. This reaction is typically

carried out in a mixed solvent system at a basic pH containing water and a miscible organic solvent [1]. The reaction coupling mechanism is shown in Figure 2.5. This suggests an overall rate expression for the coupling reaction identical to Equation 2.3, where [RNCO] is now replaced with the concentration of the isothiocyanate species.

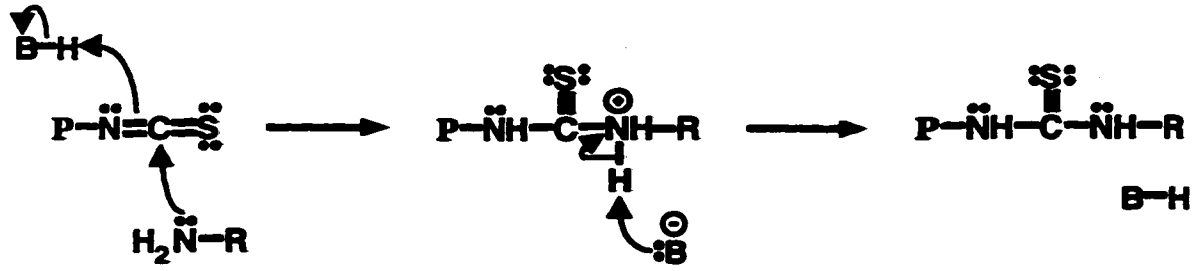

Figure 2.5: Reaction of PITC (**P**-N=C=S) with a primary amine, where **P** denotes the phenyl group and **B:** represents any available species capable of donating a proton. Adapted from [11].

However, given that the amine must be in the free base form, as in Figure 2.5, the amount of amine reactant will vary with pH [12]:

$$RNH_3^+ \overset{K_a}{\rightleftharpoons} RNH_2 + H^+ \qquad (2.4)$$

Hence it is more convenient to express the reaction rate in terms of the formal amine concentration, F_{RNH_2}:

$$F_{RNH_2} = [RNH_3^+] + [RNH_2] \qquad (2.5)$$

Substituting for $[RNH_3^+]$ using the equilibrium expression (Equation 2.4), allows RNH_2 to be expressed in terms of F_{RNH_2}:

$$[RNH_2] = \left(\frac{K_a}{K_a + [H^+]}\right) F_{RNH_2} \qquad (2.6)$$

Thus, in terms of F_{RNH_2} Equation 2.3 becomes:

$$\frac{d[\text{urea product}]}{dt} = k''_{obs} \left(\frac{K_a}{K_a + [H^+]}\right) [RNCS]\, F_{RNH_2} \qquad (2.7)$$

or

$$\frac{d[\text{urea product}]}{dt} = k'_{obs}\, [RNCS]\, F_{RNH_2} \qquad (2.8)$$

where k'_{obs} represents the observed rate constant, and k''_{obs} represents k'_{obs} when 100% of the amine is present as its free base form ($pH << pK_a$).

Thus, k'_{obs} is expected to change with pH according to Equation 2.9:

$$k'_{obs} = k''_{obs} \left(\frac{K_1}{K_1 + [H^+]}\right) \qquad (2.9)$$

where $\frac{K_a}{K_a + [H^+]} = \theta$.

In our kinetic study, the amine was present in excess (20-fold), and the reduction in the FITC peak area with time was monitored. Thus, the rate expression, as monitored, may be expressed as:

$$\frac{d[\text{FTC product}]}{dt} = k_{obs}\,[\text{FITC}] \qquad (2.10)$$

where $k_{obs} = k''_{obs}\left(\frac{K_a}{K_a + [H^+]}\right)F_{RNH_2}$ and FTC product refers to the fluorescein thiocarbamoyl product of the derivatization reaction.

An attempt was made to monitor the kinetics of lysine derivatizations; however, as the separation buffer was lowered below pH 9.28, the separation deteriorated, making any type of peak analysis impossible. This is hardly surprising given that at pH 9.28, virtually all of the ε-amino groups (95%) are protonated, whereas only slightly more than half (63%) of the α-amino groups are protonated. As the separation buffer pH is lowered, both amino groups will approach a 100% protonated state. As this occurs, their migration times would be expected to change as their relative charges change. Thus, the t-BOC (*tert*-butoxycarbonyl) protecting groups facilitated the kinetic analysis of the derivatization of each of the lysine amino groups.

k_{obs} was measured for the reaction of both Nα-t-BOC-L-lysine and Nε-t-BOC-L-lysine with FITC. The coupling of FITC with Nα-t-BOC-L-lysine occurred via the free ε-amino group and the k_{obs}'s are expressed as k_ε, whereas the coupling of FITC with Nε-t-BOC-L-lysine occurred through the free α-amino group, therefore, the corresponding k_{obs}'s are expressed as k_α.

A pH titration of the N-α- and N-ε-t-BOC-L-lysines provided an estimation of the pK_a values of their free amines. Nα-t-BOC-L-lysine's free ε-amino group was found to have a pK_a of *ca.* 10.6, while the free α-amino group of Nε-t-BOC-L-lysine had a pK_a value of *ca.* 9.4. The pK_a difference of these groups (1.2) is not as large as that of the α-

and ε-amino groups of lysine which are 1.58 pH units apart [5]. The reason for this is due to a change in the pK_a's of the α-amino groups of the two molecules, since the pK_a's of the ε-amino groups are not significantly different (10.53 and 10.6 for lysine and Nα-t-BOC-L-lysine, respectively).

Due to the smaller pK_a difference of the amino groups on the t-BOC-lysines, a plot of $\theta_\alpha / \theta_\varepsilon$ reveals less selectivity for the α-amino group relative to that predicted for lysine. $\theta_\alpha / \theta_\varepsilon$ shows that the maximum calculated selectivity for the t-BOC-lysines is half of that which may be achieved with lysine alone. Nevertheless, significant selectivity advantages are predicted on lowering the conjugation buffer pH. The pH range between 7.5 and 10.5 was investigated initially. However, the reaction occurred too rapidly at pH 10.5 to be monitored with any precision. Therefore, the pH range of 7.5-10 was studied. Linearly regressed plots of ln (FITC peak area) versus derivatization time provided correlation coefficients that were usually 0.96-0.97 (*r* value).

Isothiocyanates hydrolyze via general base catalysis in aqueous media [11,13] and produce a number of products, one of which reacts with the unhydrolyzed reagent. The reason for this is evident when the hydrolysis reaction is considered (Figure 2.6a). The isothiocyanate moiety is converted to an amino group, forming fluorescein amine, which is then free to react with unhydrolyzed FITC (Figure 2.6b). The hydrolysis rate constants for FITC will increase with pH and were therefore determined over the pH range of interest. In an effort to consider all possible hydrolysis and subsequent reaction mechanisms, the reduction in the FITC peak area with time was monitored to elucidate an observed rate constant for the loss of FITC via hydrolysis. The observed rate constants (k_{FITC}) appear in Table 2.1 with their associated errors at 95% confidence.

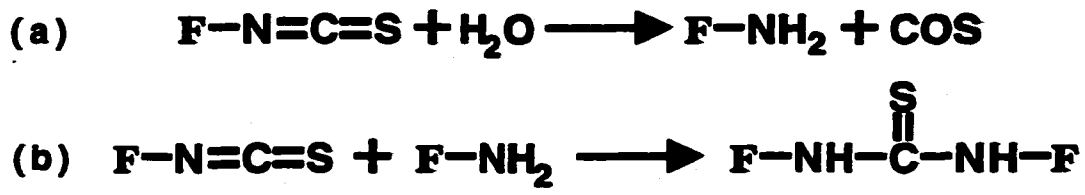

Figure 2.6: Net reactions for FITC hydrolysis, where F denotes the fluorescein group.

pH	k_{FITC} (x 10^{-4} min^{-1})
7.5	0.905 ± 0.083
8.0	1.30 ± 0.112
8.5	2.45 ± 0.138
9.0	12.2 ± 0.459
9.5	13.8 ± 2.92
10.0	26.5 ± 1.43

Table 2.1: Effective FITC hydrolysis rate constants, k_{FITC}.

A second reason for the increase in k_{FITC} with pH is that the hydrolysis reaction product, fluorescein amine, possesses an amino group that will increase in reactivity as the pH of the buffer is increased. The observed rate constants for the conjugation of FITC with Nα-t-BOC-L-lysine (k_ε) and Nε-t-BOC-L-lysine (k_α) appear in Table 2.2. Each of the k_{obs} values were corrected for FITC hydrolysis and is presented along with its associated error calculated at 95% confidence.

It is evident from Table 2.2 that both conjugation rate constants, k_α and k_ε, increase as the conjugation buffer pH is raised. However, from the ratio of k_α/k_ε in Table 2.3, it is apparent that above pH 8.0 the rate of conjugation of FITC to the ε-amino group increases faster than the rate of α-amino conjugation. In addition, relative to the standard derivatization pH range of 9.0-9.5, it is clear that a lowering of the pH should result in increased selectivity for α-amino conjugation over ε-amino conjugation.

pH	k_α (x 10^{-3} min^{-1})	k_ε (x 10^{-3} min^{-1})
7.5	0.574 ± 0.131	0.170 ± 0.0569
8.0	1.92 ± 0.622	0.393 ± 0.102
8.5	10.5 ± 0.689	2.51 ± 0.428
9.0	44.0 ± 5.81	13.1 ± 1.98
9.5	111. ± 17.3	40.1 ± 10.9
10.0	175 ± 23.5	125. ± 26.0

Table 2.2: Hydrolysis corrected effective rate constants, k_α and k_ε, for FITC derivatization with Nα- and Nε-t-BOC-L-Lysine, respectively.

Ignoring the associated error with each of the rate constants in Table 2.3, a pH of 8.0-8.5 would appear to be the optimum region for α- over ε- amino conjugation. However, when the errors are taken into consideration this is not necessarily regarded to be the case. Nevertheless, the acquired data do follow the trend that is predicted for a reaction rate dependent on the amount of the reactive form of one of the reagents. This is illustrated in Figure 2.7 where the determined values of k_α at each pH are plotted along

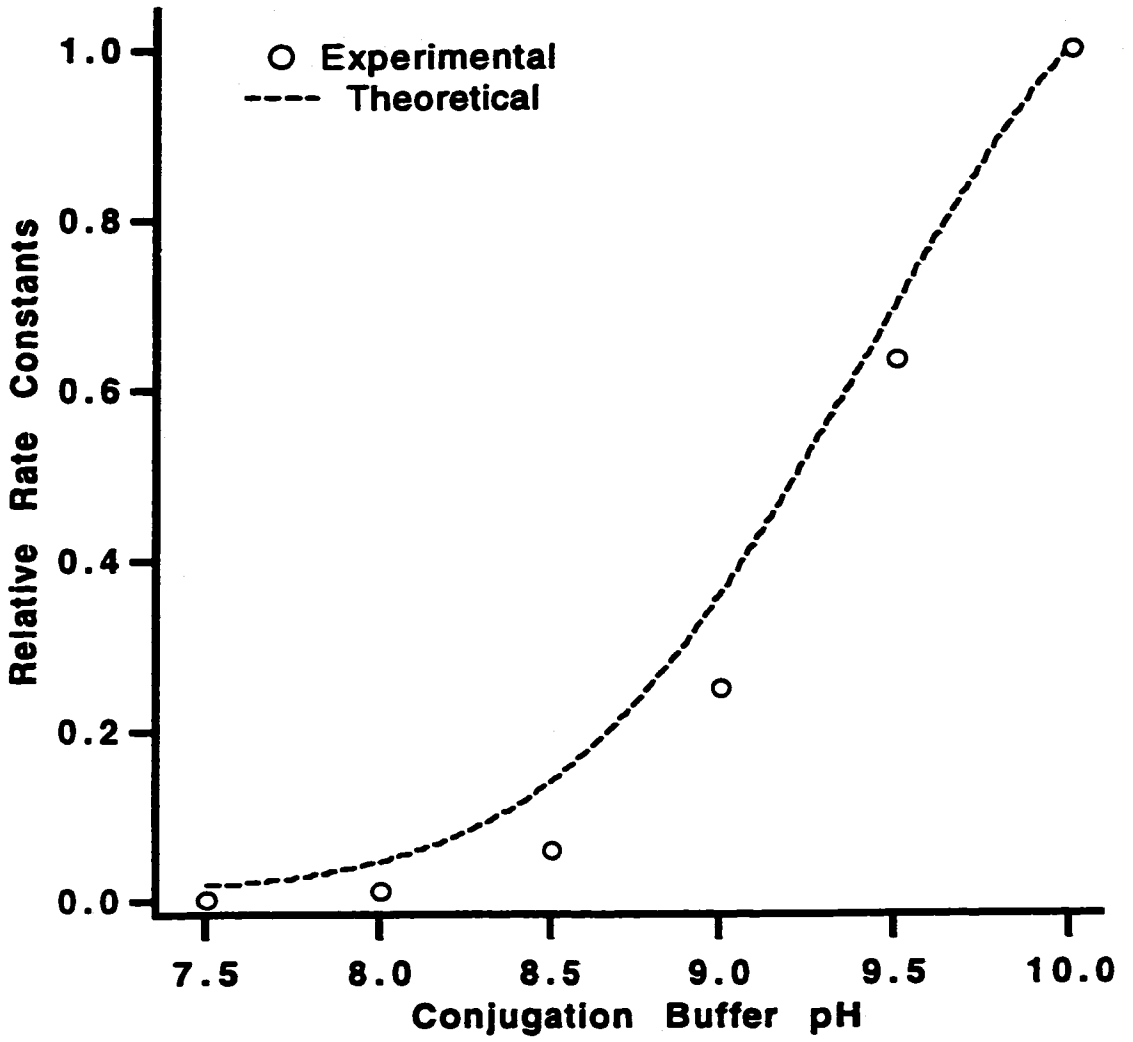

Figure 2.7: Comparison of normalized k_{obs} values for the conjugation of FITC with Nε-t-BOC-L-lysine with those expected by theory for a pH dependent reaction with a reactant possessing a pK_a of 9.4.

with those expected based on Equation 2.9 for an analyte with a reactive moiety of the same pK_a as the α-amino group of Nε-t-BOC-L-lysine, over the same pH range. Each of the theoretical and experimental effective rate constants have been normalized to their values at pH 10 to allow a facile comparison.

pH	k_α / k_ε
7.5	3.39 ± 1.37
8.0	4.89 ± 2.03
8.5	4.19 ± 0.767
9.0	3.35 ± 0.673
9.5	2.77 ± 0.870
10.0	1.40 ± 0.348

Table 2.3: Calculation of α-amino selectivity based on empirical determinations.

A comparison of the k_ε values and those calculated with Equation 2.9 for an analyte with a reactive moiety of the same pK_a as the ε-amino group of Nα-t-BOC-L-lysine possessed a similar match to one another. Therefore, given that the general trends of the effective conjugation rate constants closely those expected by theory, it may be concluded that a lowering of the conjugation buffer pH will provide an increased α-amino selectivity, as suggested by the experimentally determined data in Table 2.3.

From the results of this study, it appears that the region of pH 8.5 would be the best choice. The overall α- selectivity was found to be the largest at pH 8.0, however,

the error associated with this determination is quite large. In contrast, pH 8.5 possessed the lowest overall error (% RSD) of all of the pH's studied and, when compared to the selectivity determined at pH 8.0, the loss in potential selectivity is marginal, if any loss is occurring at all. In addition, the rate of conjugation is considerably faster at pH 8.5 requiring only 2 days to go to completion as compared to *ca.* 4-5 days for a conjugation at pH 8.0. Thus, a conjugation pH of 8.5 would be considered the optimum for the selective conjugation of a biomolecule possessing two amino groups, each with pK_a's similar to those of the t-BOC-lysines.

The goal of this work is to be able to apply the findings of the kinetic study to the routine derivatization of peptides containing multiple derivatizable amino groups. Each peptide encountered may possess amino groups with a range of pK_a values larger or smaller than those of the t-BOC-L-lysine's used as the models in this study. Therefore, the obvious conclusion is that the optimum pH for each peptide derivatization may vary. However, Creighton [14] states that 6.8-8.0 is the typical α-amino pK_a range found in proteins. The typical ε-amino pK_a range is given as 10.4-11.1. While these values are given for proteins, depending on the size of the peptide of interest and the local environment around each amino group, their amino pK_a values may fall within these ranges. It is important to note that these pKa ranges are only an approximation and a peptide of interest would have to be titrated for its amino pK_a values in order to determine whether an α-amino selectivity enhancement is possible.

The results of the pH 7.5 k_α/k_ε determination were not as expected by the $\theta_\alpha/\theta_\varepsilon$ calculation in Figure 2.3. The reason for this result is unclear, yet it is possible that at this pH a new or altered reaction mechanism has become dominant which is not as discriminatory against derivatization of the ε-amino group of the t-BOC-lysine. If the

amount of uncharged, and therefore reactive, amino groups are calculated at this pH, there are 16 times more α-amino groups capable of reacting with FITC than ε-amino groups, however, this represents a reactive α-amino concentration that is only 1.3% of all the α-amino groups.

Regardless of the mechanism, another concern that is more important to the practical use of this conjugation pH is the required reaction time. The time required for the pH 7.5 reaction to go to completion was over 7 days. This is far too long to be of any practical use for routine derivatizations. In addition, this may present problems with regard to the conjugate stability lifetime. Previous work in this laboratory has shown that at pH 9.28, the thiourea bond formed from FITC and L-lysine begins to hydrolyze at 20°C after a time period of *ca.* 2 days [4]. It is not known whether the hydrolysis is pH dependent, yet, the possibility exists that it may be self-defeating to derivatize at too low a pH as the product may begin to degrade before the reaction is complete. While, a conjugation at pH 8.0 requires only 4-5 days to go to completion, degradation of the thiourea product could still occur before any practical use of the conjugate may be made. Fortunately, the derivatizations carried out at pH 8.5 reached completion within 2 days and did not seem to exhibit any product degradation as the conjugate peak was not observed to deteriorate with time.

Aside from the obvious reason that degradation of the conjugate should be avoided as it consumes the desired product, additional considerations arise when the reaction products are examined. Figure 2.8a details the products that would be expected to be observed from the degradation of the thiourea conjugate. The thiourea bond can be cleaved such that the starting materials are regenerated, or it may be cleaved such that the

isothiocyanate and amino groups are switched [10]. In the latter case, any remaining amine reagent may now be consumed to form a dimer (Figure 2.8b) reducing further still the yield of desired fluorescent conjugate.

With the exception of the FITC hydrolysis experiments, only kinetic data that was acquired within the 2 day stability limit was used for the determination of the rate constants. Hydrolysis data was acquired for longer periods of time at pH's 7.5 and 8.0, however, the k_{obs} determinations did not seem to be affected as the % RSD values for each pH determination were 5.8 and 5.4, respectively.

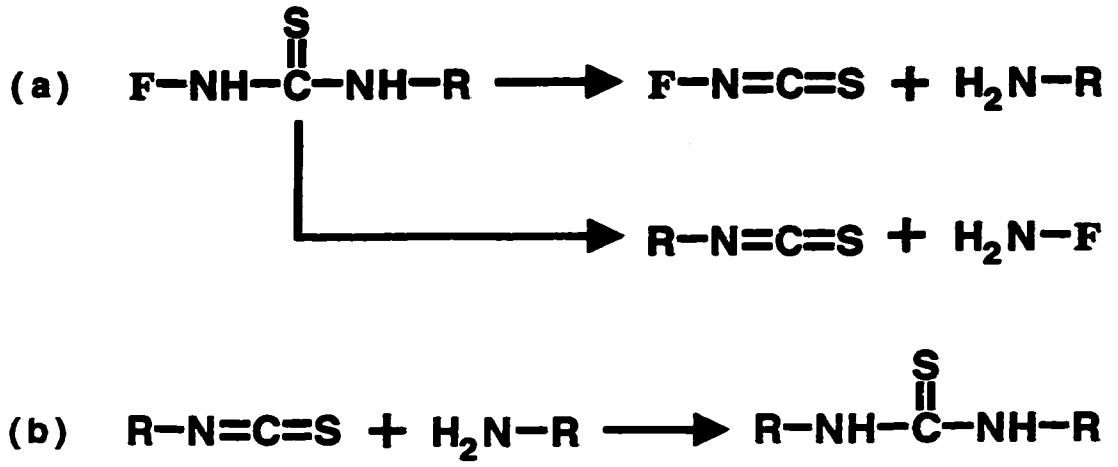

Figure 2.8: (a) Degradation of thiocarbamoyl derivative of FITC and a primary amino group
(b) Secondary reaction for consumption of primary amino group reagent.

2.4 References

1. J. Y. Zhao, K. C. Waldron, J. Miller, J. Z. Zhang, H. Harkes and N. Dovichi, *J. Chromatogr.*, 608 (1992) 239.

2. H. Maeda, N.Ishida, H. Kawauchi and K. Tuzimura, *J. Biochem.*, 65 (1969) 777.

3. W. W. Bromer, S. K. Sheehan, A. W. Berns and E. R. Arquilla, *Biochem.*, 6 (1967) 2378.

4. P. R. Banks and D. M. Paquette, *Bioconjugate Chem.*, 6 (1995) 447.

5. A. L. Lehninger, D. L. Nelson and M. M. Cox, Principles of Biochemistry, Second Ed., Worth Publishers, New York, 1993, Chapter 5.

6. H. Kawauchi, K. Tuzimura, H. Maeda and N. Ishida, *J. Biochem.*, 66 (1969) 783.

7. Fabian Zaccardo, *An Investigation into the Derivatization of α-Amines in Biomolecules using Fluorescein Isothiocyanate: Application to CZE-LIF*, P. Banks, Supervisor, Chemistry 419 Research Project, Department of Chemistry and Biochemistry, Concordia University, Montreal, PQ, 1996, p. 22.

8. R. Zahradnik, *Coll. Czech. Chem. Commun.*, 24 (1959) 3407.

9. R. Zahradnik, *Coll. Czech. Chem. Commun.*, 24 (1959) 3422.

10. D. P. N. Satchell and R. S. Satchell, *Chem. Soc. Rev.*, 4 (1975) 244-246.

11. S. N. Ege, *Organic Chemistry*, Second Ed., D. C. Heath and Company, Toronto, Ont., 1989, Chapter 26.

12. P. Zuman and R. C. Patel, Techniques in Organic Reaction Kinetics, John Wiley and Sons, Toronto, 1984, Chapter 3.

13. L. Drobnica, P. Kristian and J. Augustin, *The Chemistry of Cyanates and Their Thio Derivatives*, Part 2, S. Patai, Ed., John Wiley and Sons, Toronto, 1997, Chapter 22.

14. T. E. Creighton, Proteins: Structure and Molecular Properties, Second Ed., W. H. Freeman and Company, New York, 1993, Chapter 1.

CHAPTER 3

FLUORESCENCE DERIVATIZATION - PEPTIDE CONJUGATION STUDY

3.1 Introduction

The goal of this study was to test the conclusion of the kinetic study in Chapter 2: that a derivatization buffer of pH 8.5 may be optimum for the selective derivatization of the α-amino groups of peptides. To this end, several small peptides were chosen to be derivatized with FITC in a ratio of 1.25:1 (peptide to FITC), ensuring a slight excess of peptide to facilitate the complete consumption of FITC.

In each case, the object was to observe a single conjugate peak in the electropherogram indicative of a singly labeled analyte. If more than one label was conjugated, the electropherograms would contain additional peaks corresponding to the multiply tagged analytes. The peptides selected for this study were Arg-Lys, Lys-Trp-Lys, Lys-Lys, Lys-Lys-Lys, Lys-Lys-Lys-Lys and substance P fragment 1-4 (Arg-Pro-Lys-Pro), with each peptide possessing at least one and a maximum of four ε-amino groups.

3.2 Experimental

3.2.1 Apparatus

All electrophoretic separations were carried out using an in-house built CE-LIF system. The system employed a Spellman (Plainview, NY) model CZE1000R high voltage power supply (0-30 kV) to provide the necessary voltages for both electrokinetic

injection and electrophoretic migration. A positive potential was applied to the inlet end of the capillary, while the outlet end of the capillary was immersed in a vial containing the separation buffer. This vial was held at ground. The inlet end of the capillary was housed in an electrically-isolated polyvinyl chloride (PVC) box, to ensure operator safety. The inlet and outlet ends of the capillary were leveled in order to reduce siphoning which would influence the separation efficiency. A window was burned in the polyimide coating of the capillary approximately 10cm from the outlet end of the capillary. This window enabled on-column detection of the analytes via excitation with laser radiation, and collection of the subsequent fluorescence at 90°. The LIF setup was similar in design to that of Yeung's group [1]. Capillaries used for these separations possessed an i.d. of 50 μm and an o.d. of 186 μm, and were purchased from Polymicro Technologies (Phoenix, AZ).

The laser used in this study was a Uniphase (San José, CA) air-cooled, light-controlled 4 mW Ar^+ laser (Model 2012-4SLL). The output beam was focused onto the window of the capillary using a 6.3 X microscope objective (working distance, WD: 21mm; numerical aperture, NA: 0.20) such that the beam width was *ca.* 100 μm as it passed through the capillary. Collection was at 90° to the excitation beam using a 16 X microscope objective (WD: 3.7mm, NA: 0.32). This collection objective was fastened to a light tight box via a standard threaded microscope objective holder. The light tight box housed all the remaining components necessary for detection. Fluorescence passing through the microscope objective was focused with a biconvex lens (focal length, FL: 25.4mm) onto an iris diaphragm to spatially filter as much Rayleigh scatter as possible without significant attenuation of the fluorescence signal. Two Omega optical (Brattleboro, VT) bandpass filters (525BP15 and 535DF35) were positioned in the light

path after the iris in order to spectrally filter Raman and any remaining Rayleigh light scatter.

Detection of the spatially and spectrally filtered light, now comprised primarily of analyte fluorescence emission, was achieved with a Hamamatsu (Bridgewater, NJ) super-high-sensitivity multi-alkali photocathode photomultiplier tube (PMT) (Model R1477). The PMT possessed a peak radiant sensitivity of 80 mA W^{-1} at 450 nm, therefore, its sensitivity to fluorescein emission at 520 nm was satisfactory. The PMT was powered by a Hamamatsu high voltage power supply (model HC123-01) with an output range of -300 to -1100 V and an output to input ratio of 1000:1. The PMT voltage was always -1000 V in this study, and the resulting current from the PMT was filtered and converted to a voltage by a low-pass filter (10 MΩ resistor, 0.1 μF capacitor). The resulting voltage, proportional to the amount of fluorescence, was collected at 10 Hz using the same data acquisition board, acquisition program, analysis program as those used in the kinetic study (Chapter 2). The computer used for the data acquisition was an Apple computer (Cupertino, CA) Model Quadra 650.

3.2.2 Chemicals

Peptides Arg-Lys, Lys-Trp-Lys, Lys-Lys, Lys-Lys-Lys, Lys-Lys-Lys-Lys and substance P fragment, Arg-Pro-Lys-Pro, were obtained from Sigma (St. Louis, MO). KOH was obtained from Aldrich (Milwaukee, WI). All other reagents used were identical as those present in Chapter 2.

3.2.3 Methodology

Lys-Trp-Lys was derivatized at pH 8.5, 9.28 and pH 10. The products from each reaction were electrophoretically separated at pH 9.28. Lys-Lys, Lys-Lys-Lys and Lys-Lys-Lys-Lys were all derivatized at pH 8.5 both individually and with all three peptides together in solution. Arg-Lys and substance P fragment, Arg-Pro-Lys-Pro were derivatized at pH 8.5. The Arg-Lys FITC derivatization was a 1:1 reaction (each reagent was 1mM). All other reactions had a 1.25:1 ratio of peptide (1.25mM) to FITC (1mM). In the case of the derivatization of all three lysine peptides in solution together, a 1:1 ratio of total peptide (each peptide was 1mM) to FITC (3mM) was used. All reactions were permitted to occur for at least 12-24hr at room temperature and were repeated three times to ensure reproducibility. In each case the reaction mixture was diluted by 10^4 before fluorescence detection could be performed. Except for the Lys-Trp-Lys derivatizations all reactions were diluted with 10mM borate buffer, pH 8.5. The Lys-Trp-Lys reactions were diluted and separated in 10mM borate buffer, pH 9.28, prior to analysis. All other reactions were separated at pH 8.5 in 10mM borate/boric acid buffer.

Electrokinetic injections of 1 kV for 5 s were used for all injections which avoided sample overloading as confirmed by the symmetrical shape of the detected peaks. This represented an injection volume that was ca. 0.4 % of the total capillary volume (*ca.* 0.88 μL) for the substance P fragment derivatization separation, and an injection volume that was *ca.* 0.1 % of the total capillary volume (*ca.* 1.2 μL) for all of the other separations. The substance P fragment separation was performed at 30 kV (*ca.* 660 V/cm) while all other separations occurred at 25 kV (*ca.* 400 V/cm).

Aside from the magnitude of the applied separation voltage, all separations were identical in procedure with each step performed manually. Initially, the outside of the

capillary and the high voltage electrode were rinsed by a brief immersion in a vial containing 500μL of separation buffer. The electrode and capillary were immersed into a 500μL vial containing the sample to be analysed and the injection voltage was applied. The electrode and capillary were rinsed again with separation buffer, following which a fresh vial of separation buffer was applied and the separation voltage applied. In each case the electrophoresis was carried out until all fluoresent compounds were detected. The high voltage electrode was identical to that used in the kinetic study.

All pH titrations were carried out in an identical manner as the Nα,ε-t-BOC-L-lysine titrations in Chapter 2 except KOH was used as the titrant for each of the peptides except Arg-Lys which used NaOH as thge titrant.

The Lys-Trp-Lys electropherograms were plotted using TimeBoy, an in-house developed Igor Pro macro that permitted a normalization of all peak migration times in each electropherogram based on the migration time of a single peak common to each.

3.3 Results and Discussion

Arg-Lys has two derivatizable primary amino groups. A pH titration of the amino groups elucidated an α-amino pK_a of *ca.* 7.3 and a pK_a of *ca.* 10.1 for the ε-amino group on lysine. The pH titration curve is presented in Figure 3.1. Given that this peptide has two available amino groups for conjugation with FITC, a mixture of derivatization products is possible. Specifically, in the absence of selectivity advantages for either amino group the number of derivatization products may be determined from Equation 3.1:

$$2^n - 1 \qquad (3.1)$$

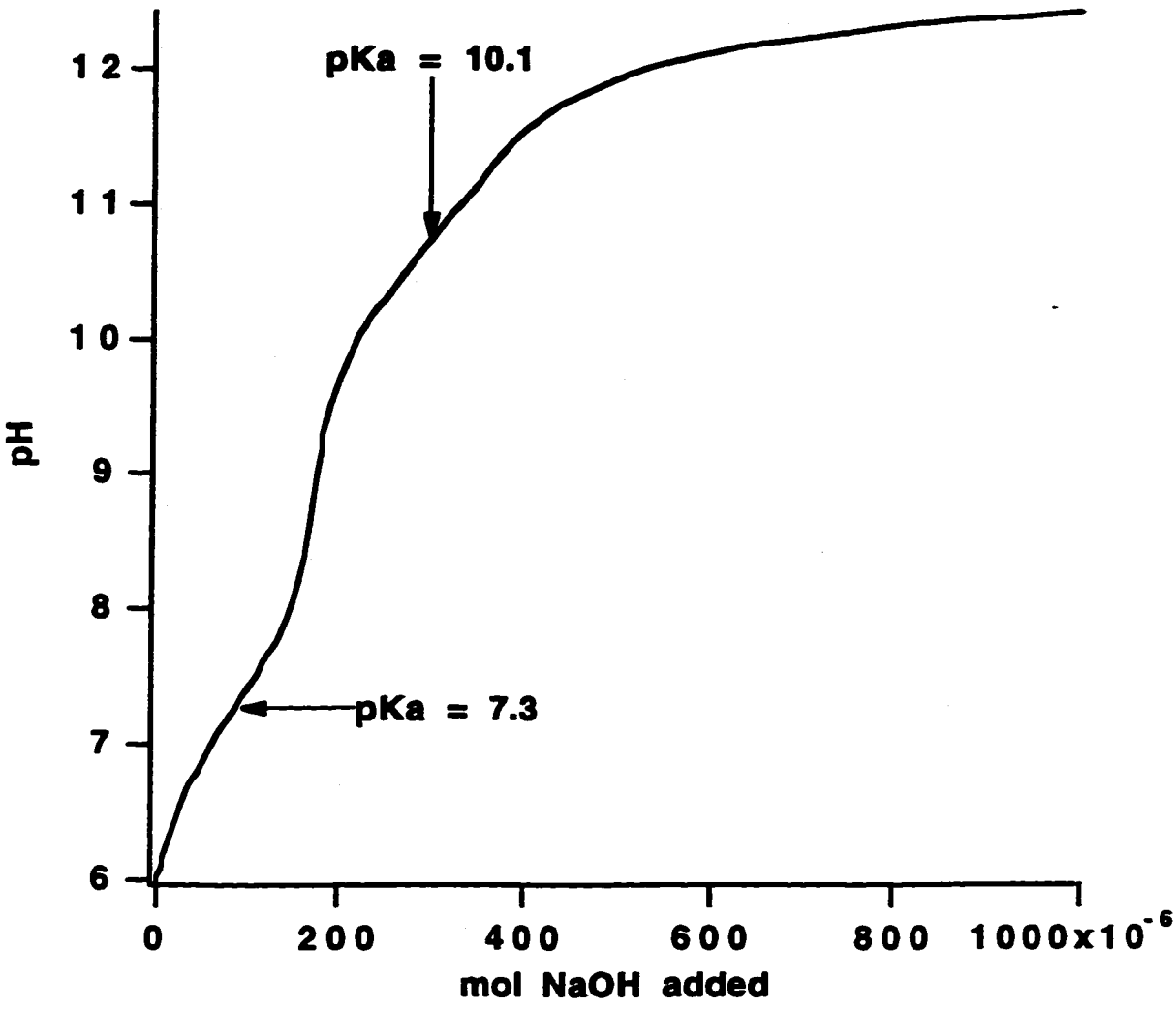

Figure 3.1: pH Titration of Arg-Lys in water with NaOH

where n = the number of derivatizable amino groups. Thus a total of 3 possible products, one with derivatization at the α-amino, one with derivatization at the ε-amino group of lysine and one with both primary amino groups derivatized. The side chain of arginine will not react with FITC since its δ-guanido group is strongly basic (pK_a *ca.* 12 for free the amino acid) and is unreactive in the protonated form [2]. Thus, the only derivatized products will be via conjugation with the available primary amino groups in their free base form.

Figure 3.2 is an electropherogram of the Arg-Lys derivatization with FITC at pH 8.5. Two of the three peaks are labeled in the figure. The largest of the three corresponds to derivatization of the N-terminal amino group. This is not surprising given that only *ca.* 2.5 % of the ε-amino groups should be present in the reactive state as compared to *ca.* 94 % of the α-amino groups. The second discernible peak in the electropherogram occurs with a migration time of 5.2min This peak was identified as unreacted FITC, while the third peak present at 5.5min is an unidentified conjugate peak, labeled either through the lysine ε-amino group or both the α- and ε-amino groups. In any event, the peak area of the α- labeled peptide is 26 times larger (peak area) than that of the second conjugate peak. The derivatization was a 1:1 reaction between FITC and the peptide. If a slight excess of peptide were used, it is likely that virtually all of the FITC would have been consumed by an N-terminal derivatization, leaving little FITC to hydrolyze or react with the other amino group.

Of interest is that the observed α-amino selectivity present in this conjugation is almost an order of magnitude greater than that observed by the kinetic study. Undoubtedly this is the result of a greater amount of uncharged α-amino groups present

on the Arg-Lys peptide as compared to the Nε-t-BOC-L-Lysine at pH 8.5. The ratio of reactive α- to ε-amino groups was *ca.* 14 for the t-BOC-L-lysines, whereas for Arg-Lys this ratio is *ca.* 38 at pH 8.5. The nucleophilicity of each of the amino groups also plays a role in the conjugations rates. For example, the kinetic study of the t-BOC-L-lysines showed that derivatization via the α-amino group had a higher observed rate constant for FITC conjugation relative to that via the ε-amino group at all pH's examined, however, as the pH increased the rate of ε-amino conjugation increased faster than that of the α-amino conjugation, decreasing the amount of α-amino selectivity. This decrease in selectivity occurred even though the number of reactive ε-amino groups was only a fraction of that of the reactive α-amino groups at each of the pH's studied, clearly demonstrating the relative nucleophilicities of the two amino groups. However, provided the pH is low enough such that there is only a small percentage of available ε-amino groups, the conjugation will occur through the α-amino group.

To further evaluate and demonstrate the enhancement in α-amino selectivity at pH 8.5, Lys-Trp-Lys was derivatized at pH's 8.5, 9.28, and 10. For analysis by CZE-LIF, each of the conjugation mixtures was diluted with 10mM borate buffer at pH 9.28. pH titration of the Lys-Trp-Lys peptide to determine its amino pK_a's was not possible due to the expense of the peptide. However, Creighton [2] lists the pK_a ranges of the α-amino and ε-amino groups found in proteins to be 6.8-8.0 and 10.4-11.1, respectively. While this peptide hardly compares in size and complexity to that of a protein, it is nevertheless reasonable to assume that the pK_a values of the amino groups should fall within these ranges. The ε-amino group pK_a value would be expected to be similar to that of the ε-amino group on Arg-Lys. Three electropherograms appear in Figure 3.3 detailing

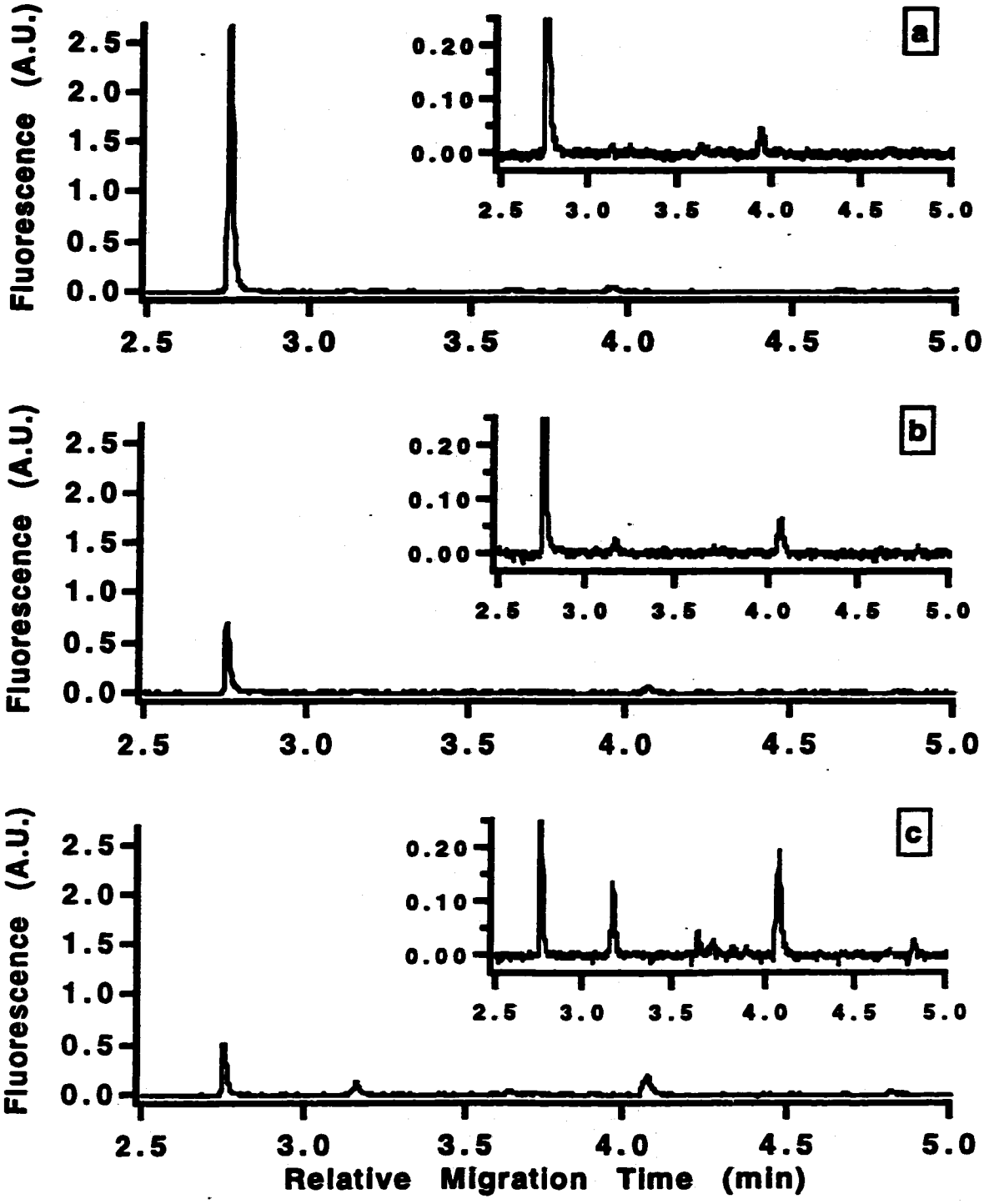

Figure 3.3: (a) Derivatization between Lys-Trp-Lys and FITC at a molar ratio of 1.25:1 at pH 8.5; (b) same reaction at pH 9.28; (c) pH 10 reaction. All derivatizations were separated at pH 9.28 by CZE-LIF.

the conjugation at each pH. For each of the electropherograms in Figure 3.3, every point has been normalized in time with respect to the migration time of the first detected compound. This allows for an easier comparison of the peaks from analysis to analysis as the migration times of the peaks can vary due to temperature fluctuations at the time of analysis.

Figure 3.3a details the pH 8.5 derivatization reaction. One major peak may be seen in the electropherogram at approximately 2.7min corresponding to the derivatization of the N-terminal amino group of the peptide. The next largest peak occurs at 3.9min and is due to the conjugation of one of the other amino groups on the peptide. The peak pertaining to the α- labeled peptide is 57 times larger (peak area) than that of the secondary conjugation peak and given that no peaks attributable to FITC hydrolysis or to FITC itself are present, this suggests that the derivatization occurred with almost 100% efficiency almost totally through the N-terminal amino group of the peptide.

Figure 3.3b details the derivatization reaction at pH 9.28. In this electropherogram it is clear that the peak attributable to the α- labeled peptide has been reduced considerably. While it is obvious that this peak has decreased in size as compared to the pH 8.5 derivatization, absolute peak heights or areas should not be compared as variations in sample injections from the manual CZE system can produce marked exaggerations when comparisons are made from run to run. Instead, comparisons of the relative peak areas within each electropherogram are more insightful as to the extent of the non α– labeling within each reaction. For example, in the pH 9.28 derivatization products, the peak attributed to the N-terminal labeled peptide is only 11 times larger than the next largest peak at 3.9min, whereas this ratio was 57 for the pH 8.5 conjugation. A third peak has now become apparent in the electropherogram with a migration time of

3.15min This peak was not detectable in the pH 8.5 derivatization and also does not correspond to that of FITC or its hydrolysis products. Thus, the amount of labeling at sites other than the N-terminus have increased over that in the pH 8.5 reaction.

Figure 3.3c shows the analysis of the derivatization which occurred at pH 10. The α- labeled peak continued to decrease while other conjugate peaks in the electropherogram increase in size. The ratio of the α- labeled peptide peak to those present at 3.15 and 3.9min are *ca.* 4 and 2, respectively. Additional peaks are apparent in the electropherogram with one present at 4.8min due to FITC hydrolysis, suggesting that hydrolysis may be a significant competitor for FITC consumption at this pH. The other peaks are due to the labeling of sites other than, or also including the N-terminus of the peptide.

Additional derivatizations were carried out using three lysine based peptides: Lys-Lys, Lys-Lys-Lys, and Lys-Lys-Lys-Lys. Lys-Lys possesses three derivatizable sites, Lys-Lys-Lys possesses four, while Lys-Lys-Lys-Lys has five. The di-lysine peptide was titrated to obtain its N-terminal pK_a and side chain ε-amino pK_a's. The N-terminal amino group was found to have a pK_a of 7.2 while the next discernible pK_a was 9.8 due one of its two ε-amino groups.

Figure 3.4 depicts the Lys-Lys derivatization with FITC. The largest peak, present at 2.5min, represents the N-terminal labeled peptide. This peak clearly dominates the electropherogram with the next largest peak (measured by peak area) at 3.7min being 31 times smaller. The next largest peak is at 3.2min and is 75 times smaller. The inset in Figure 3.4 shows the expanded region between 2.25-4.5min. Each of the peaks present correspond to a conjugation of Lys-Lys at a position other than, or in addition to, the N-terminus. Given that there are three derivatizable amino groups

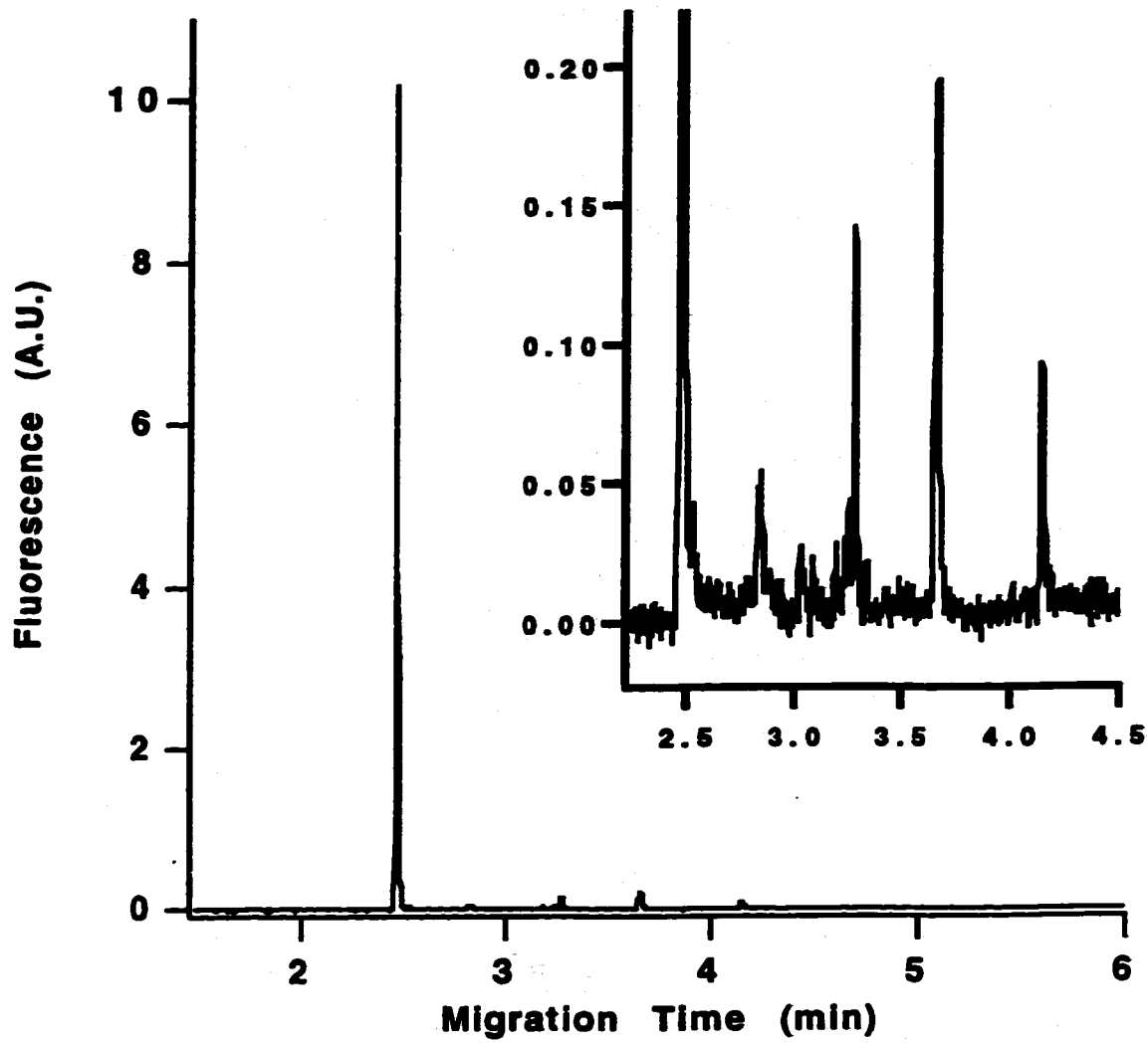

Figure 3.4: Lys-Lys derivatized with FITC in a 1.25:1 molar ratio at pH 8.5

present, a maximum mixture of 7 products is possible. Since there are six distinguishable peaks present in the mixture, almost the full compliment of derivatized products has been realized. Depending on which site is derivatized, the conjugate would be expected to have a different overall charge and hydrodynamic volume. For example, at pH 8.5 Lys-Lys would be expected to bear an overall +1 charge, two positive charges from the ε-amino groups and one negative charge from the deprotonated carboxyl group at the C-terminus. If the N-terminus was derivatized, two negative charges would be introduced into the conjugate via the carboxyl and hydroxyl moieties on the fluorescein group [3]. The resulting conjugate would be expected to have an overall charge of -1. If only one of the ε-amino groups were derivatized, an overall -2 charge on the conjugate would result. As the number of FITC labels increases on the peptide, so too does the number of negative charges; thus, for Lys-Lys with each of the available sites derivatized, the overall charge on the molecule would be -7. Given this trend, the first peak present in the electropherogram at 2.5min will correspond to derivatization of the N-terminus, as it is the only possible conjugate with an overall -1 charge. Due to the application of a positive voltage to the inlet end of the capillary, as the number of negative charges increases on the molecule, so too will its migration time, giving rise to the observed migration pattern in Figure 3.4.

Figure 3.5 shows a separation of a similar derivatization with FITC; however, the peptide employed was Lys-Lys-Lys. The relative migration times of the conjugates are expected to follow the same basic pattern as those of the Lys-Lys conjugates, with the N-terminal labeled peptide possessing the lowest overall migration time. As a result, the first peak in the electropherogram corresponds to that of the peptide labeled at the N-terminus. When a comparison is made between Figure 3.4 and 3.5, it is apparent that the

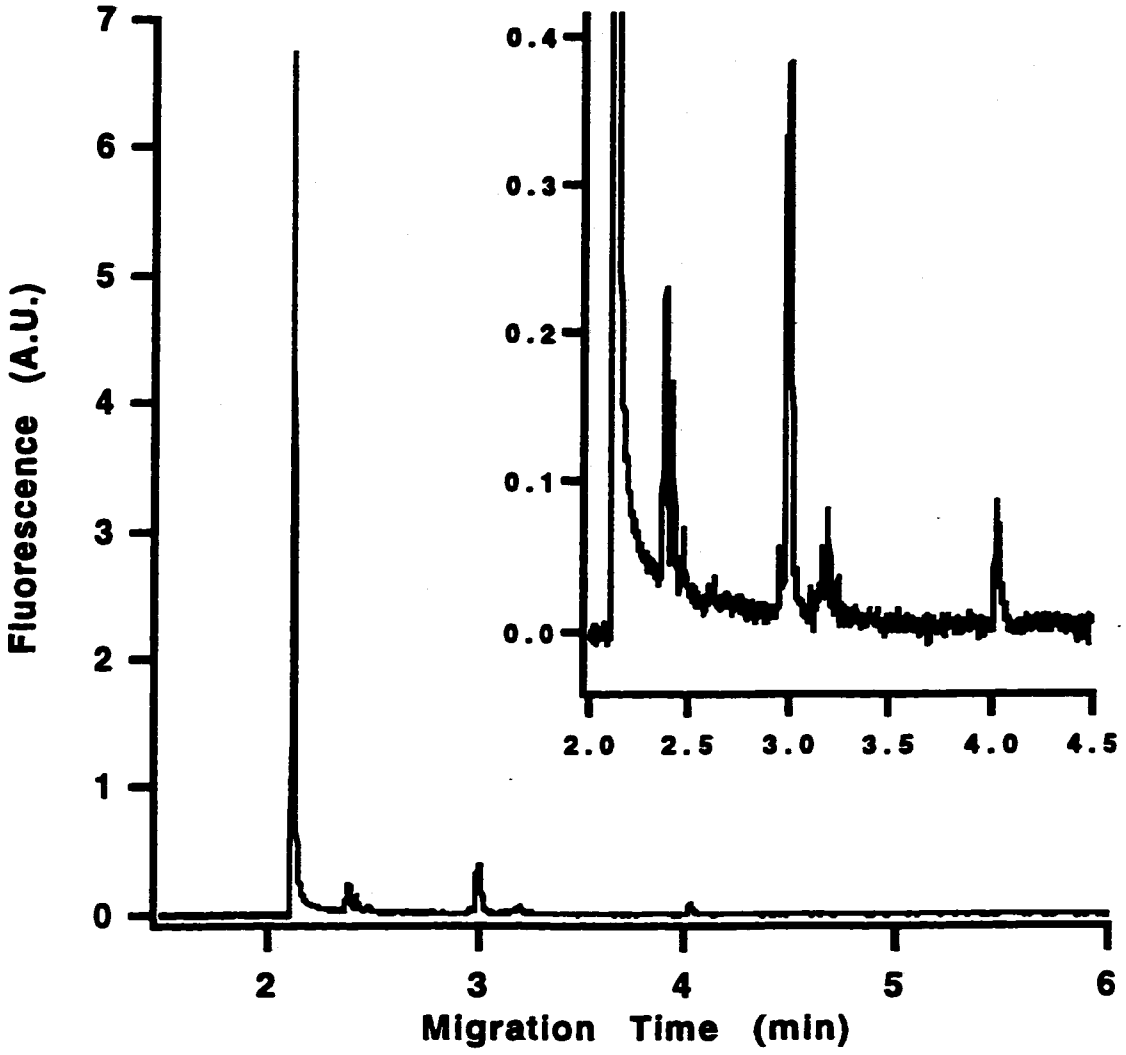

Figure 3.5: Lys-Lys-Lys derivatized with FITC in a 1.25:1 molar ratio at pH 8.5

extent of single labeling has decreased with the tri-lysine peptide. In addition to the desired product at 2.1min, there are many other peaks corresponding to other derivatization products present. Given that variations in the amount of injected sample are possible, a determination of peak area ratios further demonstrates that the amount of desired product formed has decreased with the addition of another derivatizable site. Specifically, there are five other major peaks in the electropherogram at 2.38, 2.4, 3, 3.2, and 4min A peak area ratio of the desired product to each of these peaks gives values of *ca.* 49, 180, 9.4, 80, and 69 respectively. In comparison, the N-terminus labeled peptide for the Lys-Lys derivatization was 31 times larger than the next largest peak, the corresponding ratio (9.4) for the tri-lysine conjugation is much smaller. Integration of the peaks in the electropherograms reveal that the areas of the α-labeled Lys-Lys and Lys-Lys-Lys peptide peaks are larger than the total combined areas of the other peaks present in the electropherograms by 22 and 6 fold, respectively.

The final lysine peptide studied was Lys-Lys-Lys-Lys. The derivatization conditions were the same as those for the di-lysine and tri-lysine peptides. A sample separation appears in Figure 3.6. Presumably, the largest peak in the electropherogram at 2.6min represents derivatization of the N-terminus. However, this is questionable as a single label on the N-terminus of the tetra-lysine peptide would result in an overall charge of +1 on the molecule, the highest of any of the potential conjugates. Thus, its migration time should also be the shortest, yet there are several peaks present with lower migration times than the dominate peak. It is likely that this is not a peptide conjugate labeled through the N-terminus, but rather another peptide conjugate that happens to be the most dominate form. Since the number of potential conjugates is high, it is possible that co-

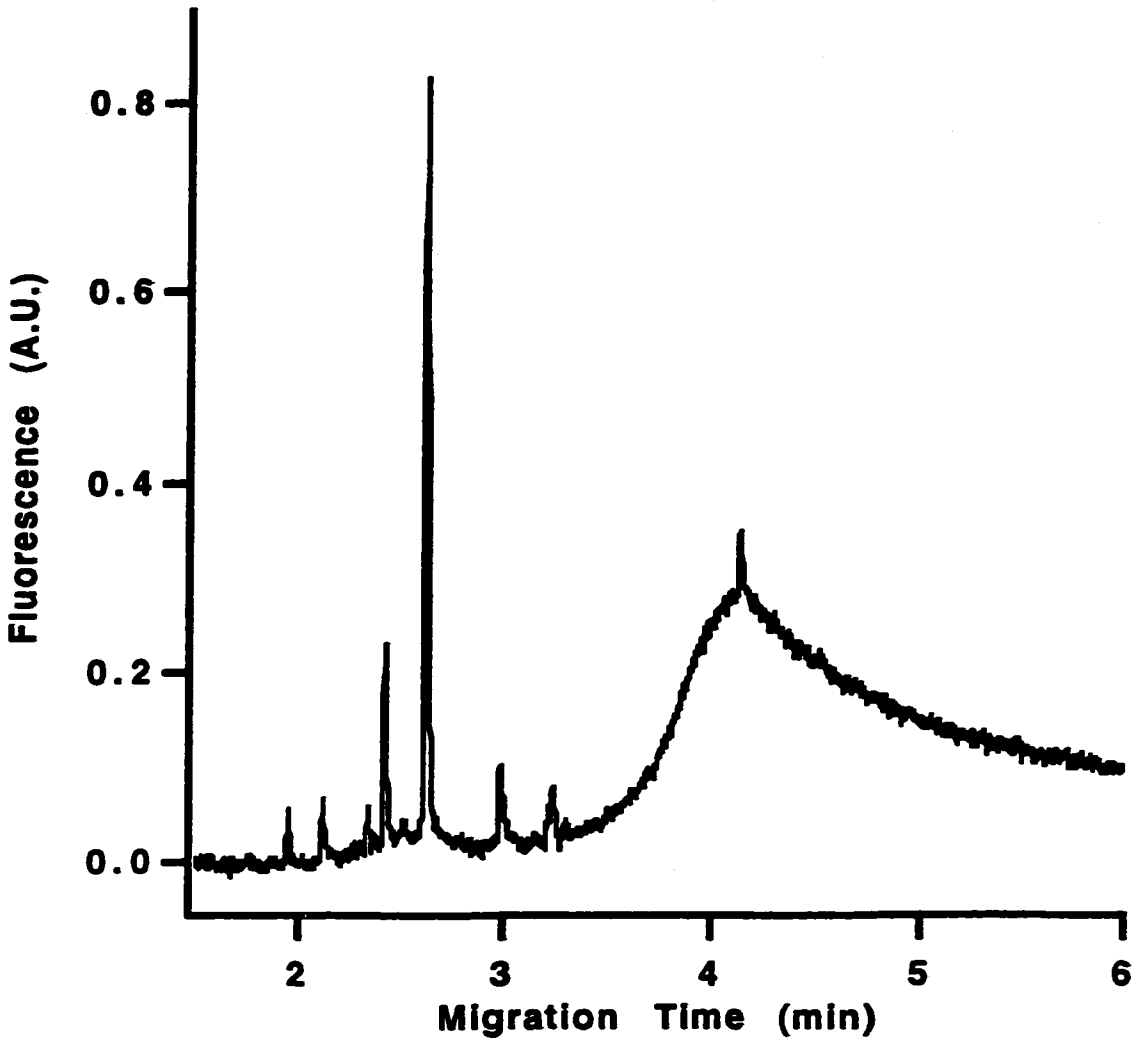

Figure 3.6: Lys-Lys-Lys-Lys derivatized with FITC in a 1.25:1 molar ratio at pH 8.5

migration of two or more species is occurring, increasing the observed peak height at 2.6min.

The addition of a fourth lysine residue has served to eliminate virtually all selective α- labeling of the peptide. Although there is the potential for up to 32 derivatized products, only 12 individual peaks may be discerned in Figure 3.6. The presence of the broadened background around 4min could be the result of several unresolved conjugates from the reaction mixture.

A titration of the tetra-lysine peptide was performed in order to determine its amino group pK_a's. The α-amino pK_a was found to be 6.7, while the next discernible pK_a was 9.4 for one or, more likely, a combination of the ε-amino groups. Thus, the observed selectivity based on amino group reactivity differences should be similar to that observed for the di-lysine peptide. However, the increased number of ε-amino groups able to compete with the α-amino group appears to reduce the overall selectivity to a level which is impractical for routine analysis. Another reason for the reduce α-amino labeling is that this amino group is not acting as a good nucleophile. This suggests that while the α-amino pK_a must be low enough such that it may be present in its free base form, it also must have a high enough nucleophilicity to act as a good nucleophile. It is possible that the α-amino group of the tetra-lysine peptide is meeting only one of these criteria.

To evaluate the derivatization method for the labeling of more than one analyte at a time, a solution containing each of the three lysine peptides was prepared and a molar amount of FITC equal to that of the total peptide concentration was added. The results are shown in Figure 3.7. The results of the conjugation closely match those of the

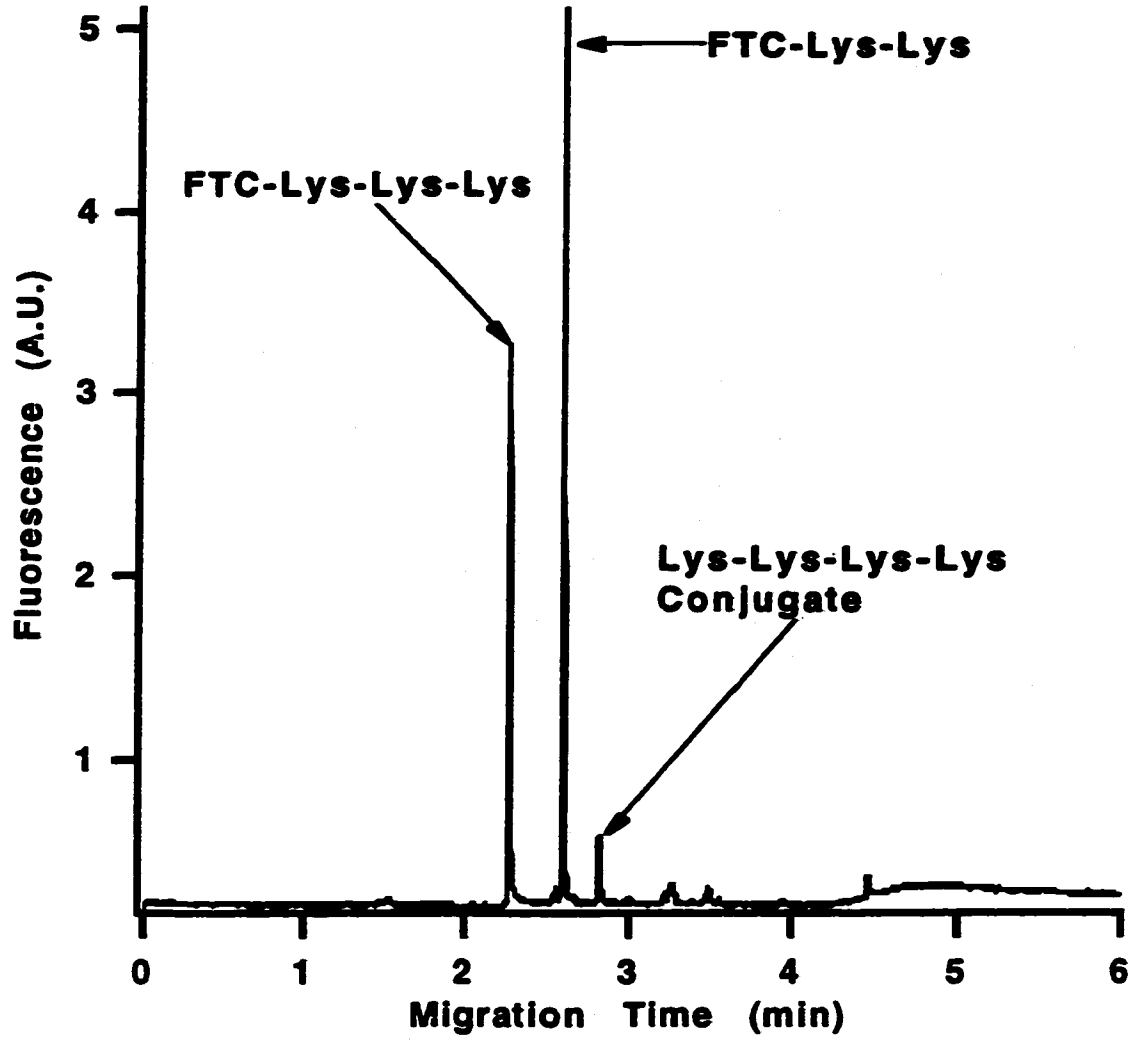

Figure 3.7: Derivatization of 1mM Lys-Lys, Lys-Lys-Lys and Lys-Lys-Lys-Lys with 3mM FITC in 0.1M borate/boric acid, pH 8.5.

individual derivatizations. For clarification, the labeled peaks were identified through spiking of the derivatization mixture with individual derivatization reactions of each peptide. This electropherogram suggests that even in samples where more than one analyte is present, it is still possible to selectively tag α-amino groups in a mixture of peptides.

A potential problem associated with this type of derivatization procedure is with regard to the amount of reagents used for the conjugation. In each study a molar ratio of either 1.25:1 or 1:1 (peptide:FITC) was used. If an excess of FITC were present, the α-amino would still be expected to derivatize first, but multiple labeling of the analyte would ultimately occur, leading to unwanted products and complicated electropherograms, e.g. Figure 3.6. While the applicability of this labeling method is limited, it may be still useful for biological studies of small molecules such as neurotransmitters and bioactive peptides. As an example, substance P fragment, Arg-Pro-Lys-Pro, was derivatized with FITC at pH 8.5. A sample electropherogram is presented in Figure 3.8 where a single peak for the derivatized analyte is present.

Based on the results presented above for each of the derivatization reactions, it is unlikely that product degradation has occurred in any of the samples. When the number of detected peaks is compared to the number of possible conjugation products, it becomes unlikely that any of these represent degradation products. However, in order to confirm this speculation a comprehensive study of thiourea product degradation at pH 8.5 would have to be carried out. Nevertheless, for each of the derivatizations at pH 8.5, with the exception of the tetra-lysine and possibly the tri-lysine conjugations, the magnitude of the other peaks in the electropherograms, relative to that of the singly α-labelled products, may be considered to be negligible.

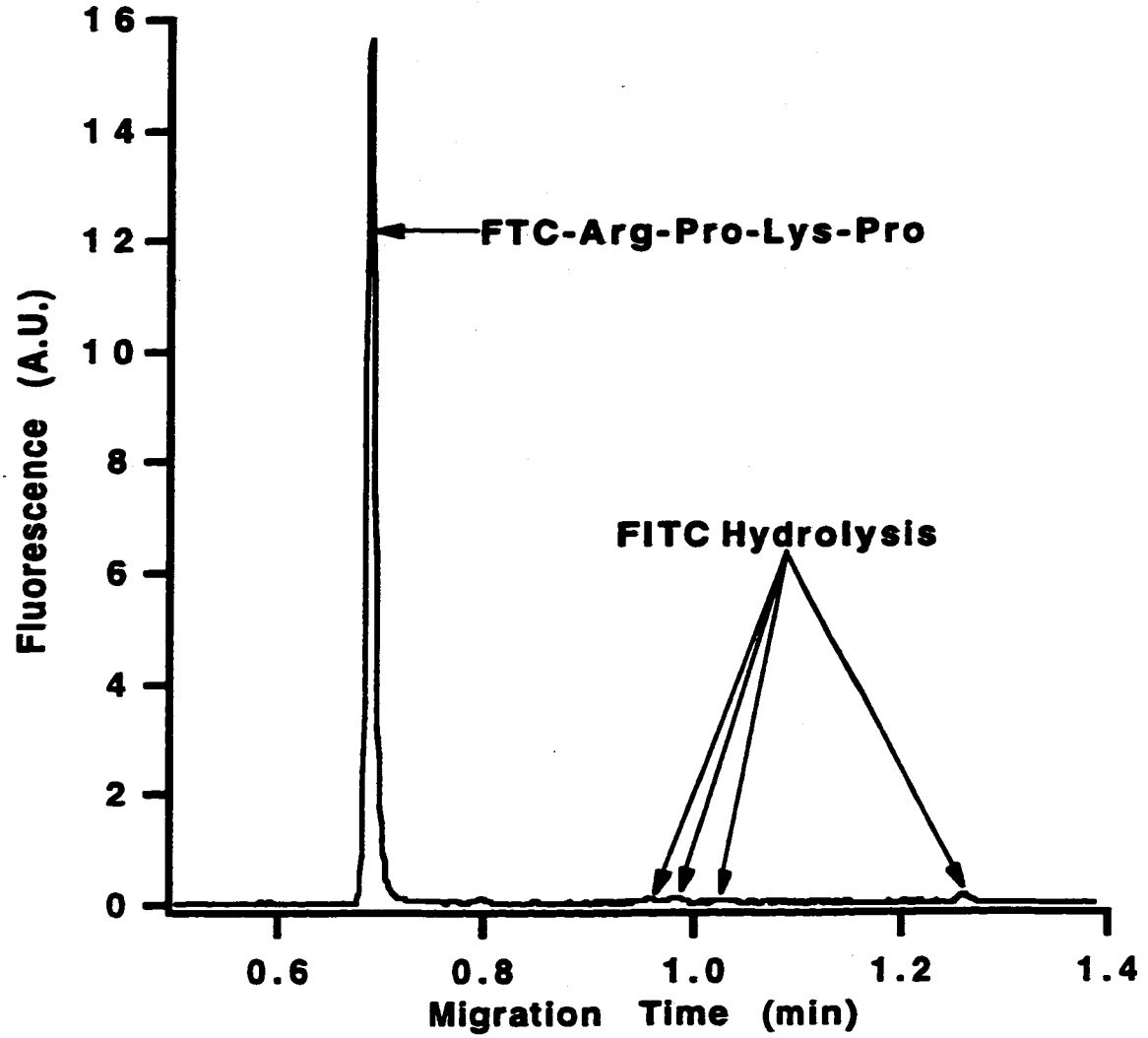

Figure 3.8: Derivatization of substance P fragment with FITC at pH 8.5.

3.4 References

1. E. Yeung, P. Wang, W. Li and R. W. Giese, *J. Chromatogr.*, 608 (1992) 73.

2. T. E. Creighton, *Proteins: Structures and Molecular Properties*, Second Ed., W. H. Freeman and Company, New York, 1993, Chapter 1.

3. N. Klonis and W. H. Sawyer, *J. Fluorescence*, 6, 3 (1996) 147.

CHAPTER 4

SUMMARY AND SUGGESTIONS FOR FUTURE RESEARCH

From the results presented in Chapters 2 and 3, the following general conclusions may be made:

A reduction of the conjugation buffer pH will result in an increased selectivity for the labeling of a peptide through its N-terminus over the labeling of any lysine side-chain ε-amino groups. Attachment of a single label is possible provided that the number of ε-amino groups is less than *ca.* 4. However, this is not a strict rule as the nucleophilicity of the N-terminal amino group will also dictate the level of observed selectivity. This was illustrated with the tetra-lysine peptide where the amount of N-terminal selectivity was observed to be the lowest of all of the peptides studied. This was partially the result of the increased number of side chain ε-amino groups on the peptide but also the result of decreased nucleophilicity of the N-terminal amino group due to the increased length of the peptide backbone relative to the other peptides studied. Thus peptides with more than three amino acid residues may not be successfully employed for single labeling unless the number of side chain ε-amino groups is lower than three.

In addition, the labeling of a mixture of the three lysine peptides suggests that a singly derivatized product may be achieved even if the analyte of interest is present in a mixture. With this a word of caution is warranted: the amount of FITC added to the sample must be judiciously controlled such that neither an excess or deficiency of the reagent exists. Either situation would lead to a non-quantitative conjugation.

However, this method of labeling may be useful for qualitative analysis of samples when one or more analytes capable of being singly labeled are present. Depending on the analyte mixture a less than equimolar amount of FITC may be required to produce a single conjugate in the electropherogram.

Perhaps the best application of the derivatization method lies with its potential use in immunoassays. Provided an antigen can be derivatized with a single label, and that the attached label will not interfere with the binding of the antigen to its antibody, this labeling method could be useful in the quantitation of immunoglobulins directed against the antigen through a direct immunoassay or, alternatively, a competitive immunoassay could be used for quantitation of the unlabeled antigen present in a sample of interest.

On the basis of the experimental results of Chapters 2 and 3, several suggestions for future study may be made. Given Satchel and Satchel's work detailing the cyclic transition state that results when the reaction between an amine and an isocyanate (and consequently an isothiocyanate) [1] occurs in an non-hydroxylic solvent, it may be of interest to study the performance of the coupling reaction in an organic solvent to determine (a) the net effect on the conjugation rate constants and, (b) the overall effect on the α- / ε- selectivity of the conjugation.

It would be of interest to perform a study on the stability of the FITC conjugate over a range of pH's. The reason for this is two-fold: (1) to determine the stability of the conjugate at pH 8.5 and (2) to determine if a lower or higher pH would result in a better overall stability of the conjugate. If so, the conjugate could be created at the pH of interest and, after derivatization is complete, the pH of the reaction mixture could be adjusted to one more appropriate for storage of the conjugate.

Finally, this project concentrated on FITC, one of the most popular fluorescent derivatization reagents. Similar studies with other fluorescent tagging reagents may elucidate better choices for conjugations through amino groups, or other possible conjugation sites.

4.4 References

1. D. P. N. Satchell and R. S. Satchell, *Chem. Soc. Rev.*, 4 (1975) 244-246.

APPENDIX I

```
|-------------------------- Macro PeakBoy ()--------------------------
|                        Written by Michael J. Little
|                              July, 1995
|-----------------------------------------------------------------------

| This macro is designed to analyze a selected peak by displaying the wave and placing
| cursor 'A' on top of the peak of interest. The file will calculate the peak height and area
| based on a fitted, calculated baseline.

| Prevents each line from being printed in command window as it is executed.
        Silent 1; PauseUpdate

| Declares variables used in program.
        Variable pos,Plates,halfheight,Tr,width,ypeak,a,b,c,n,m, integvalue, wvlength

| Ensures all waves are cleared
        KillWaves /A/Z

| Creates new wave to manipulate based on one to be analyzed.
        pos = xcsr(A)
        a = (xcsr(A)-40)
        b = (xcsr(A)+30)
        Duplicate /O/R=[a,b] wave0, wvanalysis
        SetScale/P x 0,1,"",wvanalysis

| Ensures all y values in wave are positve numbers.
        wvanalysis=wvanalysis+10

| Creates baseline based on desired selection.
        make /O/N=100 xbaseline
        make /O/N=100 ybaseline

| Selects first 10 points of desired section.
        m=0
        n=0
        do
                xbaseline(m)=(n)
                ybaseline(m)=wvanalysis(n)
```

```
            n=n+1
            m=m+1
        while (n<10)

| Selects last 10 points of desired section.
        b = numpnts(wvanalysis)
        c=(b-10)
        do
            xbaseline(m)=(c)
            ybaseline(m)=wvanalysis(c)
            c=c+1
            m=m+1
        while (c<=b)

| Redimensions baseline waves to the proper length and structure.
        Redimension /N=(30) xbaseline
        Redimension /N=(30) ybaseline

| Fits average baseline values to a line.
        CurveFit /Q line, ybaseline /X=xbaseline /D

| Calculates std dev of "baseline" values and sets peak threshold.
        WaveStats /Q ybaseline
        fit_ybaseline=(fit_ybaseline + (V_sdev*3.7))

| Compares actual signal to threshold and writes the peak only into a new wave.
        make /O/N=(numpnts(wvanalysis)) ypkhtsloc
        make /O/N=(numpnts(wvanalysis)) ypkhtsloc1
        a = 0
        do
            if (fit_ybaseline(a)<wvanalysis(a))
                ypkhtsloc(a)=(wvanalysis(a)-fit_ybaseline(a))
            endif
            a=a+1
        while ((a)<numpnts(wvanalysis))

| Adds a value of 10.025 to the wave for display purposes.
        ypkhtsloc1=ypkhtsloc + 10.025

| Finds where the peaks start and end (in points) in the new wave.
        make /O/N=2 xpkloc
        FindLevels /Q/P/M=2/D=xpkloc, ypkhtsloc, 1e-10
        c = numpnts(xpkloc)
```

```
| Finds all the "peaks" within a single peak.
        make /O/N= 10 xpeakfind
        make /O/N= 10 ypeakfind
        m = 1
        n = xpkloc(0)
        do
                FindPeak /M=1e-10/P/R=[n,(xpkloc(c)+5)]/Q ypkhtsloc
                if (V_Flag == 0)
                        xpeakfind(m) = V_PeakLoc
                        ypeakfind(m) = ypkhtsloc(V_PeakLoc)
                        n = V_PeakLoc+1
                        m = m+1
                endif
        while (V_Flag == 0)

| Checks ypeakfind to locate actual peak maxima and returns its x value position.
        n = 0
        ypeak = 0
        do
                if (ypeakfind(n)>ypeak)
                        ypeak = ypeakfind(n)
                endif
                n=n+1
        while (n<numpnts(ypeakfind))

| Locates the proper data to calculate the number of theoretical plates in the peak.
        make /O/N=2 xhalfheight
        halfheight = (ypeak/2)
        Findlevels /Q/P/M=2/D=xhalfheight, ypkhtsloc, halfheight
        width = xhalfheight(1)-xhalfheight(0)
        Tr = xcsr(A)
        Plates=5.54*((Tr/width)^2)

| Integrates new wave with peaks only.
        n=numpnts(ypkhtsloc)
        make /O/N=(n) integme
        integme=ypkhtsloc
        Integrate /T integme

| Finds Integration Values of Peaks.
        integvalue = integme(n)-integme(0)
        integme=((integme/100)+10.025)
```

```
| Displays baseline fit, new wave with peak only and original section of wave to be
analyzed.
        Display fit_ybaseline
        AppendToGraph /C=(1,4,52428) wvanalysis
        AppendToGraph /C=(0,0,0) ypkhtsloc1
        AppendToGraph /C=(2,39321,1) integme

| Print apropriate values to dialog box.
        Print "This peak was located at point number:", pos
        Print "The number of theoretical plates are:", Plates
        Print "The integration value is:  ", integvalue
        Print "The peak height is:  ", ypeak

| Deletes all variables used except those being displayed.
        KillWaves /A/Z

End
```

APPENDIX II

July, 1996

```
|-------------------------- Macro TimeBoy ()--------------------------
|                    Written by Michael J. Little
|                            July, 1996
|-----------------------------------------------------------------------
```

```
| This macro is designed to normalize every point in an acquired electropherogram to one
| common reference point. This is useful when multiple runs are being compared and
| shifts in migration times have occurred due to temperature fluctuations, etc. Placing the
| round cursor on top of the reference peak, selecting TimeBoy from the Macro menu,
| and then answering a couple experiemtal questions about the run will begin the macro.

| Declares variables used in program.
        Variable sum, freq, totalpoints,m,n,runstart,peak,runend
        Variable wavename = 1
        Variable runtime = 5
        Variable runfreq = 2

| The previous two lines create the popup menu that allows the user to input the run
| time and collection frequency used.
        Prompt runtime, "How long was each run? (in minutes)", popup
        "1;2;3;4;5;6;7;8;9;10;11;12;13;14;15;16;17;18;19;20;21;22;23;24;25;26;27;28;29;
        30;31;32;33;34;35;36;37;38;39;40;41;42;43;44;45;46;47;48;49;50;51;52;53;54;55;
        56;57;58;59;60"
        Prompt runfreq, "What collection frequency did you use? (in Hz)", popup
        "5;10;15;20;25;30;35;40;45;50"
        Prompt wavename, "What do you want the final X and Y waves to be called?",
        popup "xwave0,ywave0;xwave1,ywave1;xwave2,ywave2;xwave3,ywave3;
        xwave4,ywave4;xwave5,ywave5;xwave6,ywave6;xwave7,ywave7;xwave8,
        ywave8;xwave9,ywave9;xwave10,ywave10"

| Prevents each line from being printed in command window as it is executed.
        Silent 1; Pauseupdate

| This section properly assigns the frequency selected by the user.
        if (runfreq == 1)
                freq = 5
        endif
```

```
if (runfreq == 2)
        freq = 10
endif
if (runfreq == 3)
        freq = 15
endif
if (runfreq == 4)
        freq = 20
endif
if (runfreq == 5)
        freq = 25
endif
if (runfreq == 6)
        freq = 30
endif
if (runfreq == 7)
        freq = 35
endif
if (runfreq == 8)
        freq = 40
endif
if (runfreq == 9)
        freq = 45
endif
if (runfreq == 10)
        freq = 50
endif

| The total number of data points in the electropherogram to be analysed are calculated.
        totalpoints = freq*60*runtime
        print "The total number of data points in your electropherogram is:  ", totalpoints

| Finds the start of the wave and the position of the peak to be used to normalize the
| electropherogram.
        peak=xcsr(a)
        runstart=xcsr(b)

| Creates and scales the waves to be used to calculate the final result.
        runend=totalpoints+runstart
        make /O/N=(totalpoints) newtime
        newtime = p
        duplicate /O/R=[runstart,runend] wave0, signal
        setscale x 0,1,"", signal
```

```
| Calculates the time ratios and plots the newly adjusted wave.
        peak = peak-runstart
        newtime=newtime/peak

| This section properly assigns and displays the wave names selected for the final
| calculated waves.
        if (wavename ==1)
                duplicate /O newtime, xwave0
                duplicate /O signal, ywave0
                display ywave0 vs xwave0
        endif
        if (wavename ==2)
                duplicate /O newtime, xwave1
                duplicate /O signal, ywave1
                display ywave1 vs xwave1
        endif
        if (wavename ==3)
                duplicate /O newtime, xwave2
                duplicate /O signal, ywave2
                display ywave2 vs xwave2
        endif
        if (wavename ==4)
                duplicate /O newtime, xwave3
                duplicate /O signal, ywave3
                display ywave3 vs xwave3
        endif
        if (wavename ==5)
                duplicate /O newtime, xwave4
                duplicate /O signal, ywave4
                display ywave4 vs xwave4
        endif
        if (wavename ==6)
                duplicate /O newtime, xwave5
                duplicate /O signal, ywave5
                display ywave5 vs xwave5
        endif
        if (wavename ==7)
                duplicate /O newtime, xwave6
                duplicate /O signal, ywave6
                display ywave6 vs xwave6
        endif
        if (wavename ==8)
```

```
        duplicate /O newtime, xwave7
        duplicate /O signal, ywave7
        display ywave7 vs xwave7
    endif
    if (wavename ==9)
        duplicate /O newtime, xwave8
        duplicate /O signal, ywave8
        display ywave8 vs xwave8
    endif
    if (wavename ==10)
        duplicate /O newtime, xwave9
        duplicate /O signal, ywave9
        display ywave9 vs xwave9
    endif
    if (wavename ==11)
        duplicate /O newtime, xwave10
        duplicate /O signal, ywave10
        display ywave10 vs xwave10
    endif

End
```